NOAA Technical Memorandum ERL AOML-69

SURFACE METEOROLOGICAL AND NEAR SURFACE OCEANOGRAPHIC ATLAS OF THE TROPICAL INDIAN OCEAN

R. R. Rao
R. L. Molinari
J. F. Festa

Atlantic Oceanographic and Meteorological Laboratory
Miami, Florida
June 1991

noaa NATIONAL OCEANIC AND ATMOSPHERIC ADMINISTRATION / Environmental Research Laboratories

NOAA Technical Memorandum ERL AOML-69

SURFACE METEOROLOGICAL AND NEAR SURFACE OCEANOGRAPHIC ATLAS OF THE TROPICAL INDIAN OCEAN

R. R. Rao
Physical Oceanographic Division
Naval Physical and Oceanographic Laboratory
Cochin, India

R. L. Molinari
J. F. Festa
Atlantic Oceanographic and Meteorological Laboratory

Atlantic Oceanographic and Meteorological Laboratory
Miami, Florida
June 1991

UNITED STATES
DEPARTMENT OF COMMERCE

Robert A. Mosbacher
Secretary

NATIONAL OCEANIC AND
ATMOSPHERIC ADMINISTRATION

John A. Knauss
Under Secretary for Oceans
and Atmosphere/Administrator

Environmental Research
Laboratories

Joseph O. Fletcher
Director

NOTICE

Mention of a commercial company or product does not constitute an endorsement by NOAA/Environmental Research Laboratories. Use of information from this publication concerning proprietary products or the tests of such products for publicity or advertising purposes is not authorized.

For sale by the National Technical Information Service, 5285 Port Royal Road
Springfield, VA 22161

CONTENTS

SURFACE METEOROLOGICAL AND NEAR SURFACE OCEANOGRAPHIC ATLAS OF THE TROPICAL INDIAN OCEAN

R. R. Rao, R. L. Molinari, and J. F. Festa

ABSTRACT. Historical observations of surface marine meteorology (COADS: 1950-1979), near surface vertical thermal structure (MOODS: 1948-1981), and near surface ship drift (Cutler and Swallow, 1984: 1854-1974) for the tropical Indian Ocean are compiled to generate mean monthly climatologies of several observed and derived parameters on a 2° × 2° grid. The derived parameters include surface heat exchanges, surface wind stress and its curl, mixed layer depth (MLD), vertical thermal gradient just beneath the mixed layer, depth of 20°C isotherms, and zonal and meridional near surface flow patterns. The formulations used in the derivation of these quantities are also presented. The resultant climatological fields are machine contoured. The annual cycle of many of the fields are presented in terms of amplitude and phase of the annual and semi-annual harmonics.

1. INTRODUCTION

The tropical oceans appear to play a key role in modulating global atmospheric processes. With the occurrence of anomalous ENSO events leading to large scale global droughts and floods, for instance, the importance of air-sea interactions in the tropical oceans has gained increased interest in recent years. International research programs such as the Tropical Oceans and Global Atmosphere (TOGA) and the World Ocean Circulation Experiment (WOCE) have been developed to study the role of the ocean in climate variability. Unfortunately, relatively meager data are available for studies of tropical areas compared to extra-tropical regions.

The tropical Indian Ocean, with its unique seasonal reversing monsoons, forms an integral part of TOGA and WOCE research programs. Although small in dimension in comparison with its counterpart tropical Pacific Ocean, it is landlocked in the north and represents an area of intense air-sea interaction under the influence of seasonal reversing monsoons and transient cyclonic storms.

This atlas contains descriptions of the annual cycle of surface meteorological elements, surface heat flux estimates, surface wind stress and its curl, mixed layer depth, depth of 20° isotherms (representative of the thermocline), and near surface ship drift current vectors for the entire tropical Indian Ocean. The intent of this atlas is to provide a more complete description of the annual cycle of the air-sea interaction parameters/processes, subsurface thermal structure, and near surface circulation for the entire tropical Indian Ocean. The monthly fields presented here are computer generated from the monthly data on a 2° latitude by 2° longitude grid. This atlas provides an integrated description of the observed annual cycle in the tropical Indian Ocean in the context of global ocean-atmosphere interactions. A portion of the data have been presented in Rao et al. (1989).

2. DATA AND DATA PROCESSING

2.1 Surface Marine Meteorological Data

The data used to compute the surface fields presented in this atlas come from the Comprehensive Ocean-Atmosphere Data Set (COADS) (Woodruff et al., 1987). The COADS is one of the largest and most complete data sets of marine data available today. Ramage (1987) points out that the COADS wind data have larger mean scalar winds during the 1950-1979 period than for the earlier 1900-1939 period. This trend is probably due to changes in measurement techniques. Because of this trend and other possible inaccuracies, as well as the limited amount of data available before 1950, this atlas is only based on the 1950-1979 period. Monthly averages of all standard marine meteorological parameters on a 2° by 2° grid for the period 1950-1979 have been kindly provided by Dr. Scott D. Woodruff as a subset of Comprehensive Ocean Atmosphere Data Set (COADS). The details of input data sets, data volume, data reduction and storage, quality control are presented elsewhere (Slutz et al., 1985; Woodruff et al., 1987).

Mean monthly climatologies of SST, surface meteorological variables and surface energy fluxes based on COADS data already exist (Shea, 1986; Sadler et al., 1987a; Wright, 1988; Oberhuber, 1988a). Several factors justify the effort required to reconstruct similar fields. The period 1950-1979 is characterized by high density data coverage. In addition, this data set is more homogeneous than earlier data sets since the measurement techniques did not change during this period. However, the data distribution clearly shows a bias for major international shipping routes (Figure 1). The resulting monthly climatologies of surface wind vectors are given in Figures 2, 3 and 4; sea-surface pressure, Figures 5, 6 and 7; surface air temperature, Figures 8, 9 and 10; surface specific humidity, Figures 11, 12 and 13; total cloudiness, Figures 14, 15 and 16; and sea-surface temperature, Figures 17, 18 and 19.

2.2 Subsurface Temperature Data

The climatological description of the subsurface temperature distribution for the tropical Indian Ocean is based on relatively fewer observations than are available for other oceans (Wyrtki, 1971; Colborn, 1975; Robinson et al., 1979; Levitus, 1982). The subsurface temperature data for this study were provided by the Fleet Numerical Oceanographic Center as the Master Oceanographic Data Set (MOODS). The MOODS data set consists of CTDs, BTs and hydrocasts collected between 1948 and 1981. Approximately 25,000 temperature profiles in the eastern tropical Indian Ocean were added to the 50,000 profiles considered by Molinari et al. (1986) in the western Indian Ocean to generate a basin-wide climatology. In the present study, the mixed layer depth (MLD) is defined as the first depth at which the temperature is 1.0°C less than that at 10 m depth. A review of the vertical temperature gradients just below the mixed layer indicates that over most of the basin these gradients were greater than 2°C/20 m. Thus, the MLD estimates would, in general, not be sensitive to order of 1°C changes in this criterion. The depth of the 20°C isotherm (D20) is chosen to represent the depth of the thermocline, as this isotherm is typically present in the thermocline over most of the basin.

Mixed layer depth and depth of 20°C isotherm values were derived from individual profiles. The MLD and D20 values were then averaged on a 2° latitude by 2° longitude grid, first by day, to reduce the influence of multiple

data collected in the same day, and then by month. When sufficient data existed, a biased sample variance was computed for a grid point. A mean standard error of the mean for the entire domain was then determined by averaging the variances. Differences between mean daily and mean monthly values were computed at each point. Daily values more than two standard errors different from the mean monthly values were deleted and new monthly means were then computed.

Monthly data distributions are shown along with mixed layer depth distributions. Regions outside of the main shipping lanes have few available data. A 9-point Laplacian estimator was used as a final check for outliers, particularly in these areas. To fill in grid points where no data were available, a method similar to the smoothing-spline method of Ooyama (1987) was used. The particular technique applied here is described in detail in Thacker (1987). The resulting MLD (Figures 20, 21 and 22) and D20 (Figures 23, 24 and 25) climatologies are generated and machine contoured.

2.3 Ship Drift Vector Data

The ship drift data were obtained from the United Kingdom Meteorological Office archives of historical surface currents. Observations extend through the period 1854 to 1974. The area covered is bounded by the coasts of Asia and Africa, longitudes 50°E (in the Gulf of Aden) and 100°E, and latitude 25°S. Cutler and Swallow (1984) compiled these surface currents into 10-day periods and 1 degree quadrangles of latitude and longitude. For each 10-day period and 1 degree quadrangle, the vector mean of all the observations from all years has been estimated. To reduce the temporal and spatial noise further, the data are averaged on 2° latitude by 2° longitude boxes for each month. The number of observations in each 2° box is given in Figure 26. The mean monthly climatological distribution of the observed ship drift vectors are given in Figures 27, 28 and 29.

2.4 Surface Flux Data

The individual flux terms needed to estimate the net surface flux are typically derived from the bulk aerodynamic formulas. The bulk exchange coefficients are functions of near surface stability, measurement height, surface wind speed and sea state. The problems associated with the use of the bulk formulae are numerous and well documented (Blanc, 1985, 1987; Molinari and Hansen, 1986). For instance, Sarachik (1984) notes that the two basic problems with these formulae are calibration and data. The various functions and coefficients are determined by "regressing these formulas against high quality measurements as can be taken on shipboard" (Sarachik, 1984). However, the calibration data are very limited. Thus, in the case of exchange coefficients "there is now no single, universally accepted bulk transfer coefficient scheme" (Blanc, 1985).

Reed's (1977) comparisons for typical tropical shortwave fluxes (order of 100-200 W/m^2) imply errors greater than 20 W/m^2. These uncertainties are greater than the TOGA requirement for shortwave radiation estimates. Similar difficulties are encountered when estimating net longwave radiation. For instance, Hastenrath and Lamb (1978) assume a weaker reduction due to cloud cover than does Bunker (1976) or Reed (1983), resulting in larger longwave fluxes (of the order of 50%) (Reed, 1983).

Blanc (1985) reviewed ten pulished bulk transfer coefficient schemes and finds that differences in latent and sensible heat fluxes related to different schemes are frequently large [0 (100%)]. Bunker (1976) used a variety of sources, most of which used indirect measurements to constrain a tabular coefficient scheme. The coefficients are tabulated as a function of wind speed and stability. The latent and sensible heat coefficients are assumed equal. In general, the Bunker coefficients at neutral stability were the largest considered by Blanc (1985). Large and Pond (1982) determined different latent and sensible heat flux coefficients by indirect observations. Both are considerably less than the Bunker coefficients. Hastenrath and Lamb (1978) used a constant drag coefficient of 1.4×10^{-3} for both latent and sensible heat fluxes.

Herein, the mean monthly surface data and the bulk aerodynamic formulas given by Molinari et al. (1985) are used, with one difference, to estimate the four components of net surface heat flux. The sensible and latent heat fluxes are computed here using the variable exchange coefficients given by Bunker (1976) rather than the constant value used by Molinari et al. (1985).

The net shortwave, Q_{sw}, and longwave, Q_{LW}, radiation (in W/m^2) are estimated using the following equations:

$$Q_{sw} = 0.94\, Q_o\, (1.0 - 0.38c - 0.38\, c^2)$$

$$Q_{LW} = \varepsilon\sigma\, T_s^{\,4}\, (0.39 - .056\, \sqrt{q_a})\, (1 - 0.53\, c^2) + 4\varepsilon\sigma\, T_s^{\,3}\, (T_s - T_a)$$

The sensible, Q_s, and latent, Q_e, heat fluxes (in W/m^2) are estimated using the following bulk aerodynamic formulations:

$$Q_s = \rho\, C_D\, c_p\, (T_s - T_Q)\, V$$

$$Q_e = \rho\, C_D\, L\, (q_s - q_a)\, V$$

where

ρ = density of air ($1.175\ kg/m^3$)

C_D = exchange coefficient (after Bunker, 1976)

C_p = specific heat of air (1.012 KJ/kg/°C)

T_s = air temperature (°K)

T_a = sea surface temperature (°K)

V = scalar wind speed (m/s)

q_s = saturation specific humidity at T_s (g/kg)

q_a = specific humidity at T_a (g/kg)

L = latent heat of vaporization ($2484 - 2.39 \times T_s$) kJ/kg

Q_o = clear sky radiation (after Budyko, 1963)

c = fractional cloud cover (after Berliand, 1960)

Q_{LW} = net longwave radiation (after Berliand and Berliand, 1952)

ε = emissivity (1)

σ = Stefan-Boltzman's constant (567×10^{-10} $W/m^2/K^4$)

Mean monthly distributions of shortwave (direct solar) radiation balance, Q_{sw}, are given in Figures 30, 31 and 32; net longwave radiation, Figures 33, 34, and 35; sensible heat flux, Figures 36, 37 and 38; and latent heat flux, Figures 39, 40 and 41. The net surface heat flux, Q, is computed as

$$Q = Q_{sw} - Q_{LW} - Q_s - Q_e.$$

Mean monthly distributions of net heat gain are given in Figures 42, 43 and 44.

3. DISCUSSION

Using the estimates for uncertainty in the surface meteorological variables given in Table 1 and a propagation of error analysis (Meyer, 1975), error estimates for individual flux terms are equivalent to an uncertainty in net surface flux of 10 W/m^2 within the shipping lanes and about 25 W/m^2 outside the shipping lanes. However, these errors are independent of any inadequacies of the bulk fomulas and depend only on sampling and instrumental uncertainties.

Table 1. Ensemble average standard error of the mean values for 2° × 2° quadrangles within the shipping lanes (450 values) and outside shipping lanes (300 values).

Element	Unit	450 Values	300 Values
Sea surface temperature	°C	0.1	0.3
Sea level pressure	(mb)	0.2	0.9
Air temperature	(°C)	0.0	0.2
Wind speed	(m/s)	0.3	0.9
Specific humidity	(gms/Kg)	0.1	0.4
Cloud cover	(tenths)	0.2	0.6
Shortwave radiation	(W/m^2)	5.2	18.0
Net longwave radiation	(W/m^2)	1.2	4.3
Sensible heat flux	(W/m^2)	1.0	3.7
Latent heat flux	(W/m^2)	7.8	23.9

Estimates of the amplitude and phase of the first two (i.e., annual and semi-annual) harmonics of the annual cycle for various oceanic properties were also computed. Amplitudes are expressed both in terms of property units and the percent of total variance accounted for by each harmonic. Phases are given in months with respect to 0 phase on 15 January. The amplitudes and phases for sea surface temperature are given in Figure 45; for mixed layer depth, Figure 46; for 20°C topography, Figure 47; and for the zonal and meridional components of surface current in Figures 48 and 49, respectively.

4. REFERENCES

Berliand, M. E., and T. G. Berliand, 1952. Measurement of the effective radiation of the earth with varying cloud amounts (in Russian). Izv. Akad. Nauk SSSR Ser. Geofiz., No. 1.

Berliand, T. G., 1960. Method of climatological estimation of global radiation. Meteor. Gidrol., 6:9-12.

Blanc, T. V., 1985. Variation of bulk-derived surface flux, stability, and roughness results due to the use of different transfer coeficient schemes. J. Phys. Oceanogr., 15:650-669.

Blanc, T. V., 1987. Accuracy of bulk-method-determined flux, stability and sea surface roughness. J. Geophys. Res., 92(C4):3867-3876.

Budyko, M. I., 1963. Atlas of the Heat Balance of the Earth. Gidrometeorozdat, Leningrad, 69 pp.

Budyko, M. I., 1984. Climate and Life. Academic Press, New York, 508 pp.

Bunker, A. F., 1976. Computations of surface energy flux and annual air-sea interaction cycles of north Atlantic Ocean. Mon. Weather Rev., 104:1122-1140.

Colborn, J. G., 1975. The Thermal Structure of the Indian Ocean, IIOE Oceanographic Monographs, No. 2. University of Hawaii Press, Honolulu, HI, 173 pp.

Cutler, A., and J. Swallow, 1984. Surface currents of the Indian Ocean (25°S, 100°E). Complied from historical data archieved by the Meteorological Office, Bracknell, UK Institute of Oceanographic Sciencies, Rept. No. 187 (8 pp. and 36 charts).

Hastenrath, S., and P. Lamb, 1978. Heat Budget Atlas of the Tropical Atlantic and Eastern Pacific Oceans. University of Wisconsin Press, Madison, WI, 104 pp.

Large, W. G., and S. Pond, 1982. Sensible and latent heat flux measurements over the ocean. J. Phys. Oceanogr., 12:464-482.

Levitus, S., 1982. Climatogical Atlas of the World Ocean. NOAA Professional Paper, No. 13, U.S. Gov't. Printing Office, 173 pp.

Meyer, S. L., 1975. Data Analysis for Scientists and Engineers. John Wiley, New York, 513 pp.

Molinari, R. L., J. F. Festa, and J. C. Swallow, 1985. Evolution of sea-surface temperature and surface meteorological fields in the tropical Atlantic Ocean during FGGE, 1979. Prog. Oceanogr., 14, 401-420.

Molinari, R. L., J. F. Festa, and J. C. Swallow, 1986. Mixed layer and thermocline depth climatologies in the Western Indian Ocean. NOAA Tech. Memo. ERL AOML-64, NOAA Atlantic Oceanographic and Meteorological Laboratory, Miami, FL, 40 pp.

Molinari, R. L., and D. V. Hansen, 1988. Observational studies of near surface thermal budgets in the tropics: review, evaluation and recommendations. U.S. TOGA Workshop Report on the Dynamics of the Equatorial Oceans, Honolulu, HI, 450 pp.

Oberhuber, J. M., 1988. An atlas based on the COADS data set: the budgets of heat, buoyancy, and turbulant kinetic energy at the surface of the global ocean. Max-Planck Institute of Meteorology, Rept. No. 15, Hamburg.

Ramage, C. S., 1987. Secular changes in reported surface wind speeds over the ocean. J. Clim. Appl. Meteorol., 26:525-528.

Rao, R. R., R. L. Molinari, and J. F. Festa, 1989. Evolution of the climatological near-surface thermal structure of the tropical Indian Ocean. 1. Description of mean monthly mixed layer depth, and sea surface temperature, surface current and surface meteorological fields. J. Geophys. Res., 94, 10,801-10,815.

Reed, R. K., 1977. On estimating insolation over the ocean. J. Phys. Oceanogr., 7:482-485.

Reed, R. K., 1983. Heat fluxes over the tropical Pacific Ocean. J. Clim. Appl. Meteorol., 24:833-840.

Robinson, M. K., R. A. Bauer, and E. H. Schroeder, 1979. Atlas of Atlantic-Indian Ocean monthly mean temperatures and mean salinities of the surface layer. Naval Oceanographic Office, Reference Pub. No. 18, Dept. of the Navy, Washington, D.C., 213 pp.

Sadler, J. C., M. A. Lauder, A. M. Hori, and L. K. Oda, 1987a. Tropical Marine Climatic Atlas, Vol. I, Indian Ocean and Atlantic Ocean. University of Hawaii, UHMET, 87-01, 51 pp.

Sarachik, E. S., 1984. Large-scale surface heat fluxes. In Large-Scale Oceanographic Experiments and Satellites. C. Gautier and M. Fieux (Eds.), D. Reidel Publishing Co., Boston, 147-165.

Shea, D. J., 1986. Climatological Atlas: 1950-1979. National Center for Atmospheric Research, Boulder, CO.

Slutz, R. J., S. L. Lubker, J. D. Hiscox, S. D. Woodruff, R. L. Jenne, D. H. Joseph, P. M. Steuver, and J. D. Elms, 1985. Comprehensive ocean-atmosphere data set: Release 1. NOAA Environmental Research Labs., Climate Research Program, Boulder, CO, 268 pp.

Woodruff, S. D., R. J. Slutz, R. L. Jenne, and P. M. Steuver, 1987. A comprehensive ocean-atmosphere data set. Bull. Amer. Meteorol. Soc., 68, 1239-1250.

Wright, P. B., 1988. An atlas based on the COADS data set: fields of mean wind, cloudiness and humidity at the surface of the global ocean. Max-Planck Institute for Meteorology, Rept. No. 14, Hamburg.

Wyrtki, K., 1971. Oceanographic atlas of the International Indian Ocean Expedition. National Science Foundation, Washington, D.C., 531 pp.

5. LIST OF FIGURES

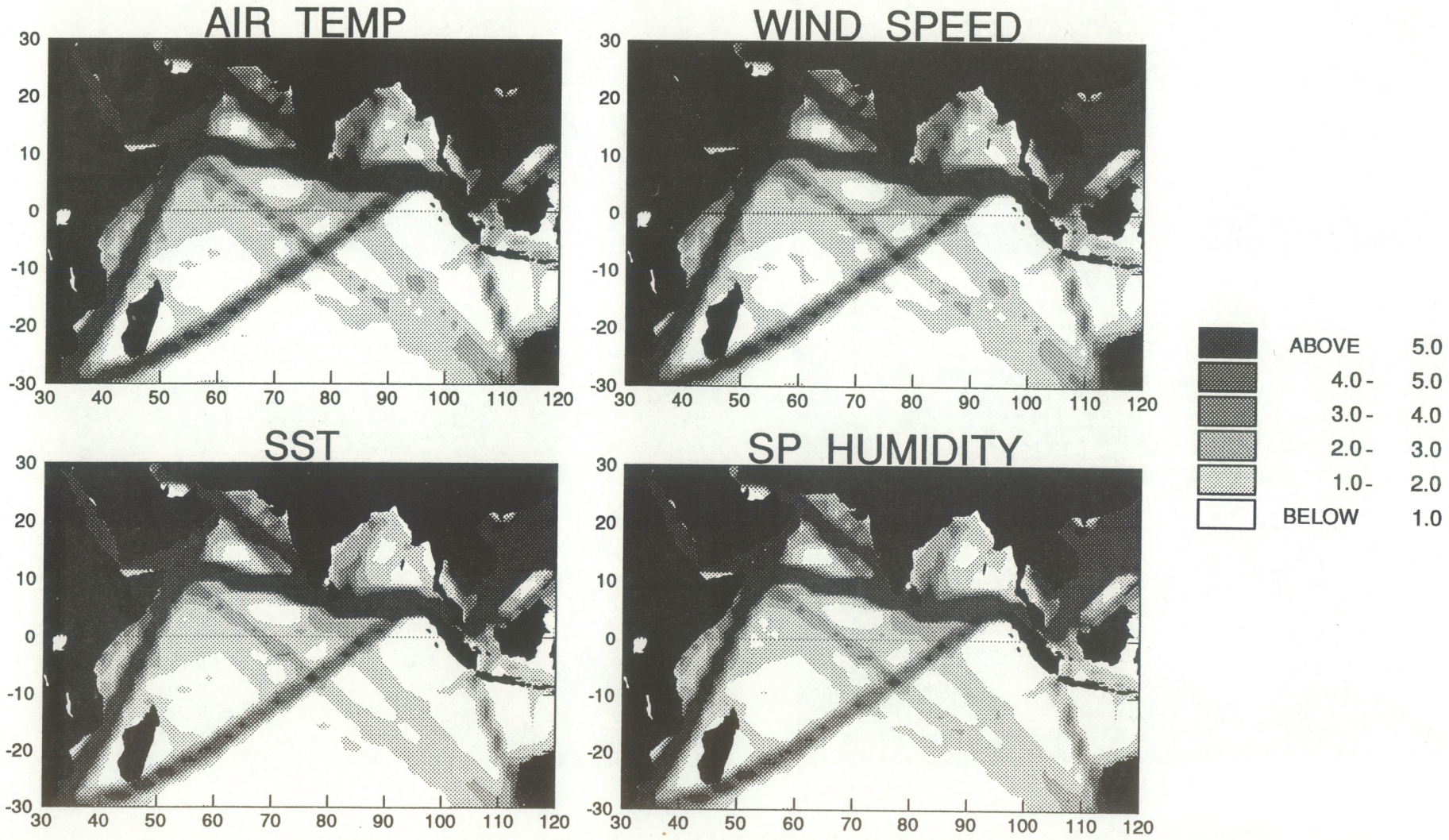
COADS OBSERVATIONS(1950-79) IN THOUSANDS
AIR TEMP
WIND SPEED
SST
SP HUMIDITY
30
20
10
0
-10
-20
-30
30 40 50 60 70 80 90 100 110 120
ABOVE 5.0
4.0 - 5.0
3.0 - 4.0
2.0 - 3.0
1.0 - 2.0
BELOW 1.0

Figure 1

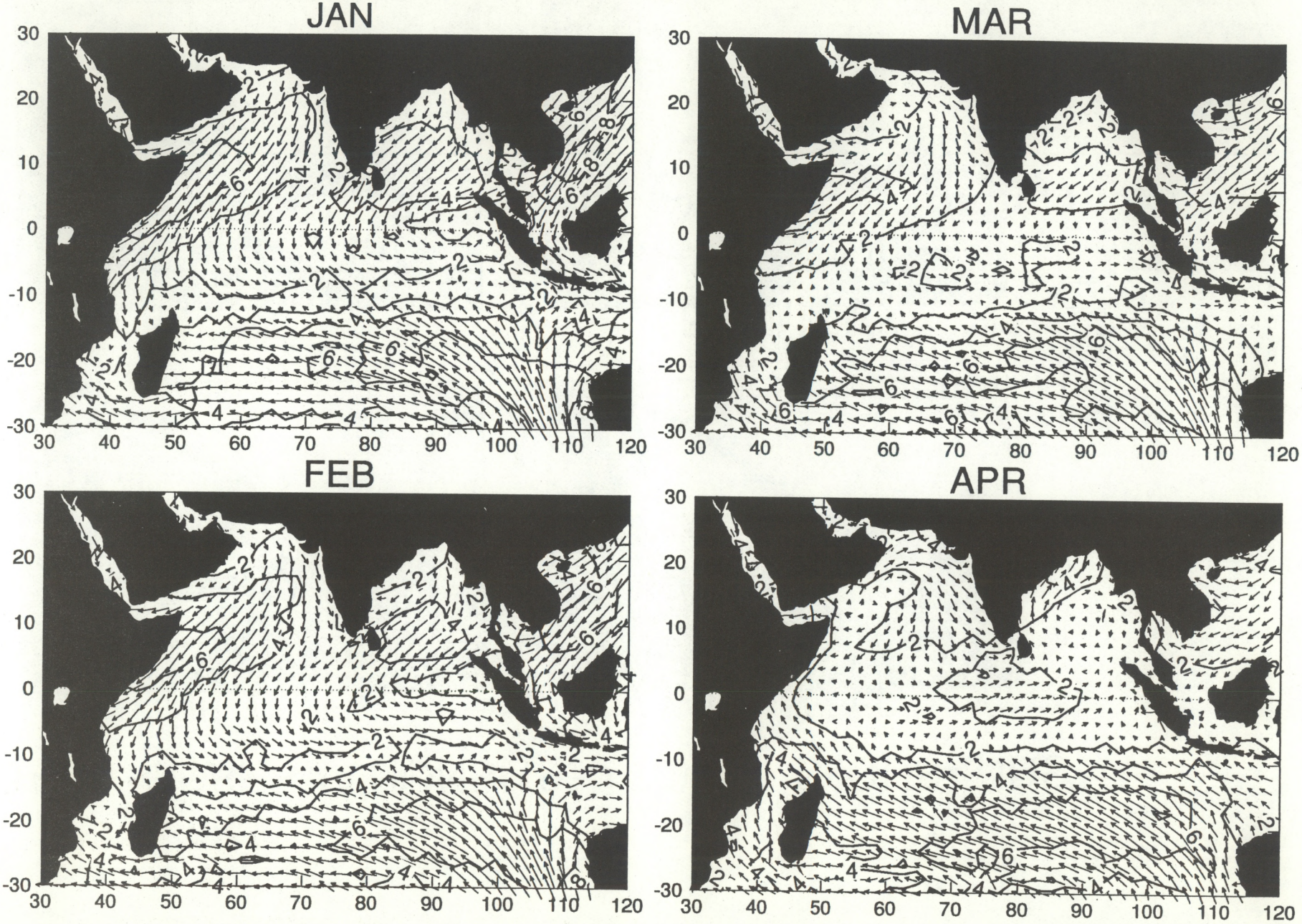

Figure 2

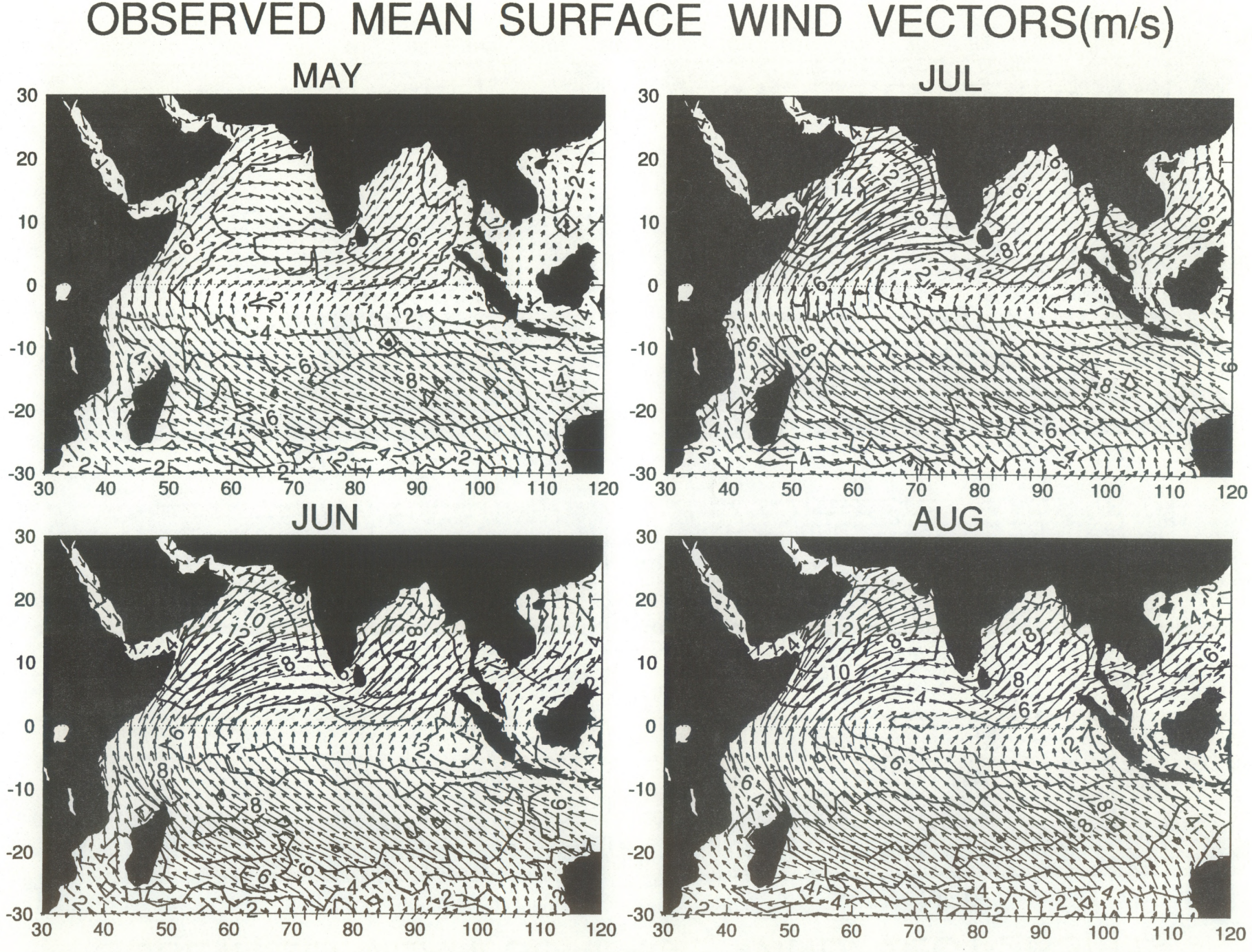
OBSERVED MEAN SURFACE WIND VECTORS(m/s)
MAY
JUL
JUN
AUG
30
20
10
0
-10
-20
-30
30 40 50 60 70 80 90 100 110 120

Figure 3

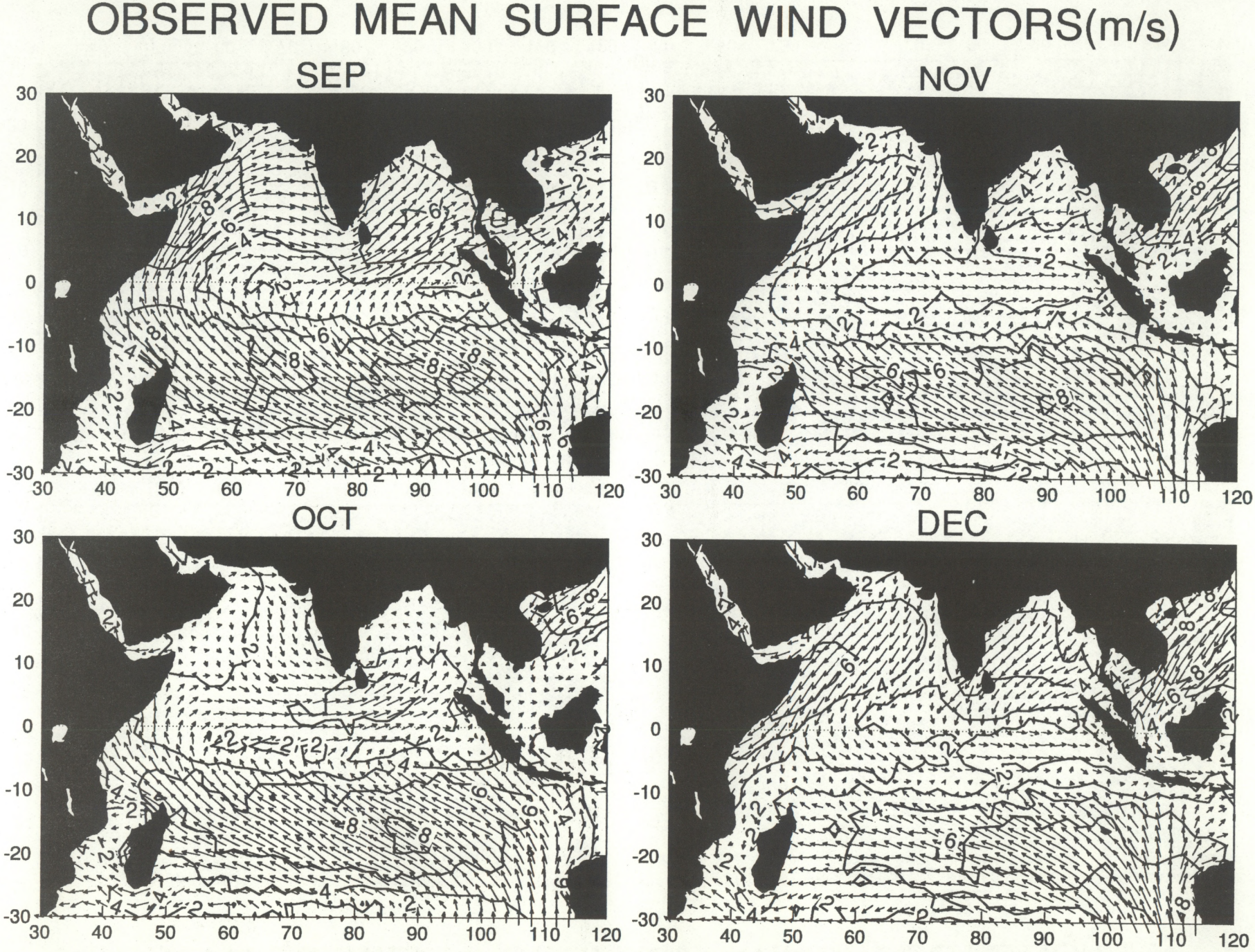

Figure 4

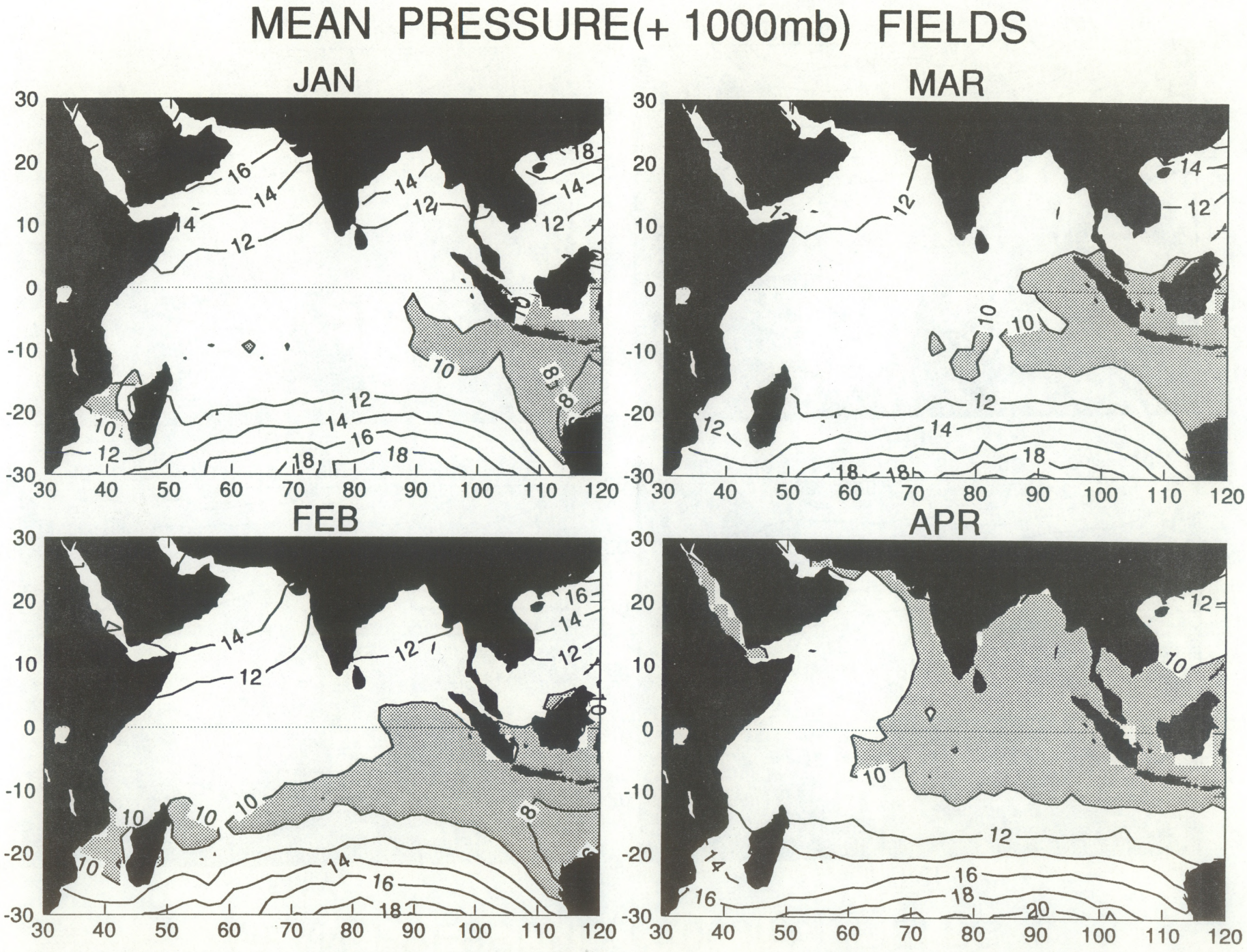

Figure 5

MEAN PRESSURE(+ 1000mb) FIELDS

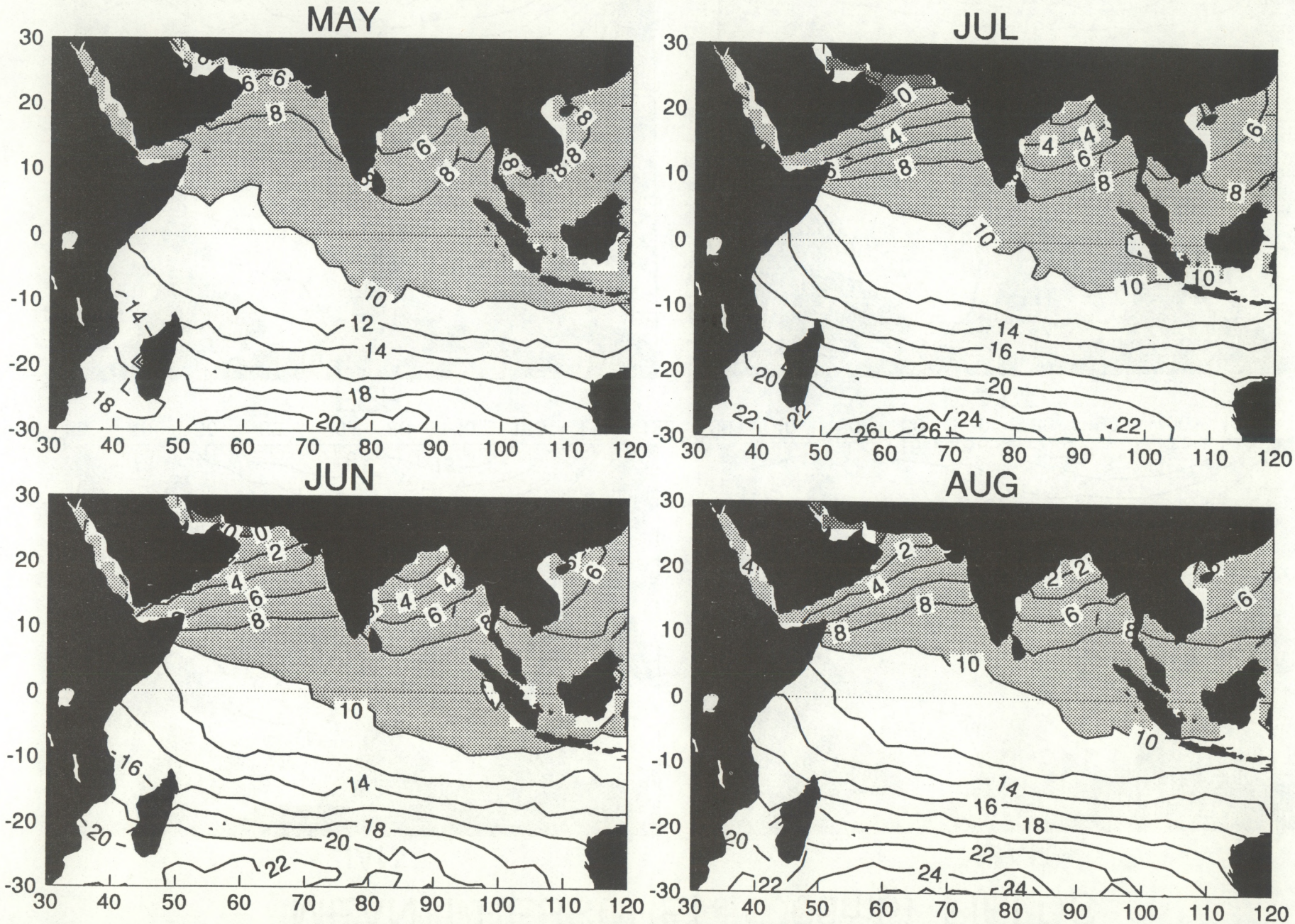

Figure 6

MEAN PRESSURE(+ 1000mb) FIELDS

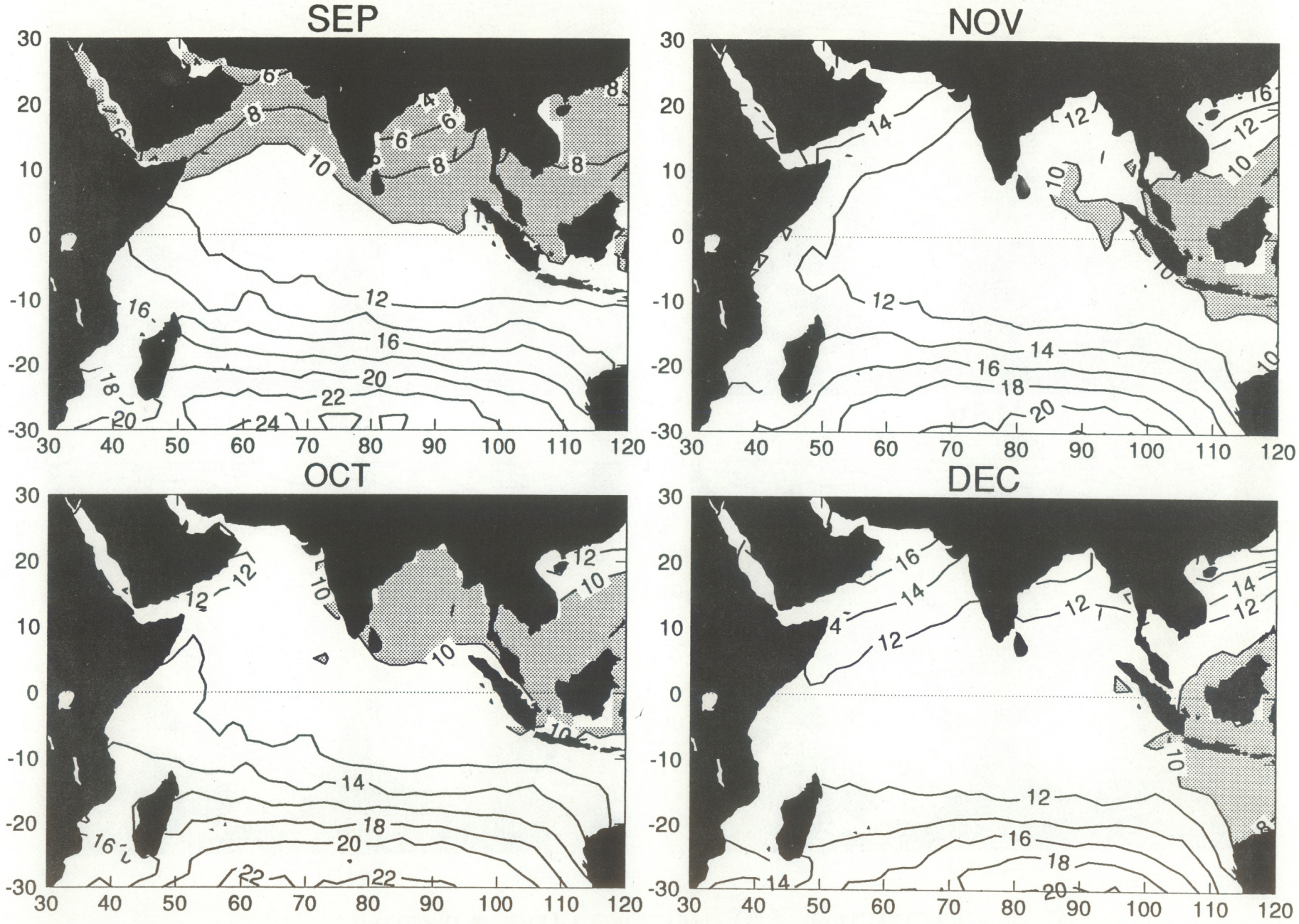

Figure 7

MEAN AIR TEMP(c) FIELDS

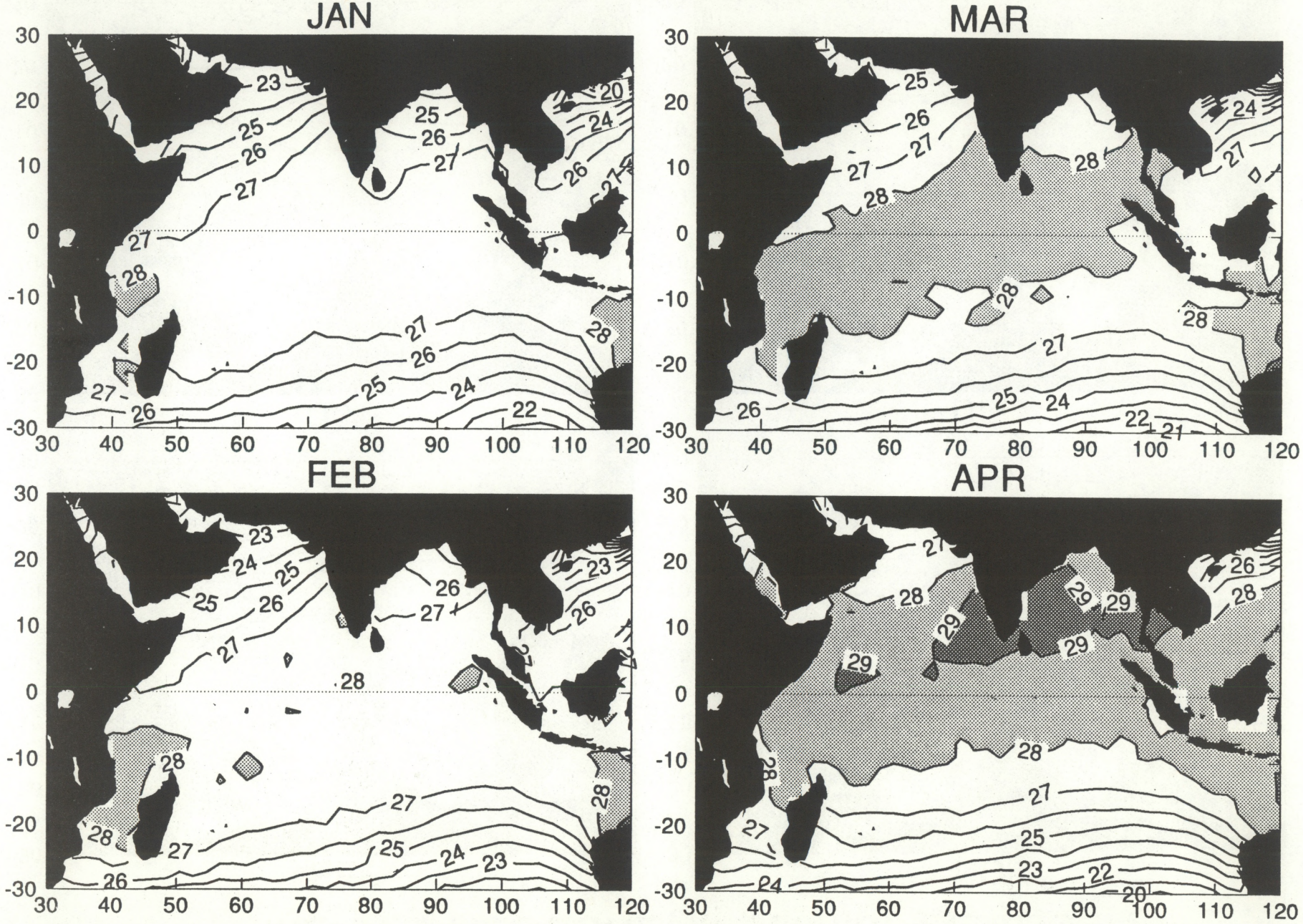

Figure 8

MEAN AIR TEMP(c) FIELDS

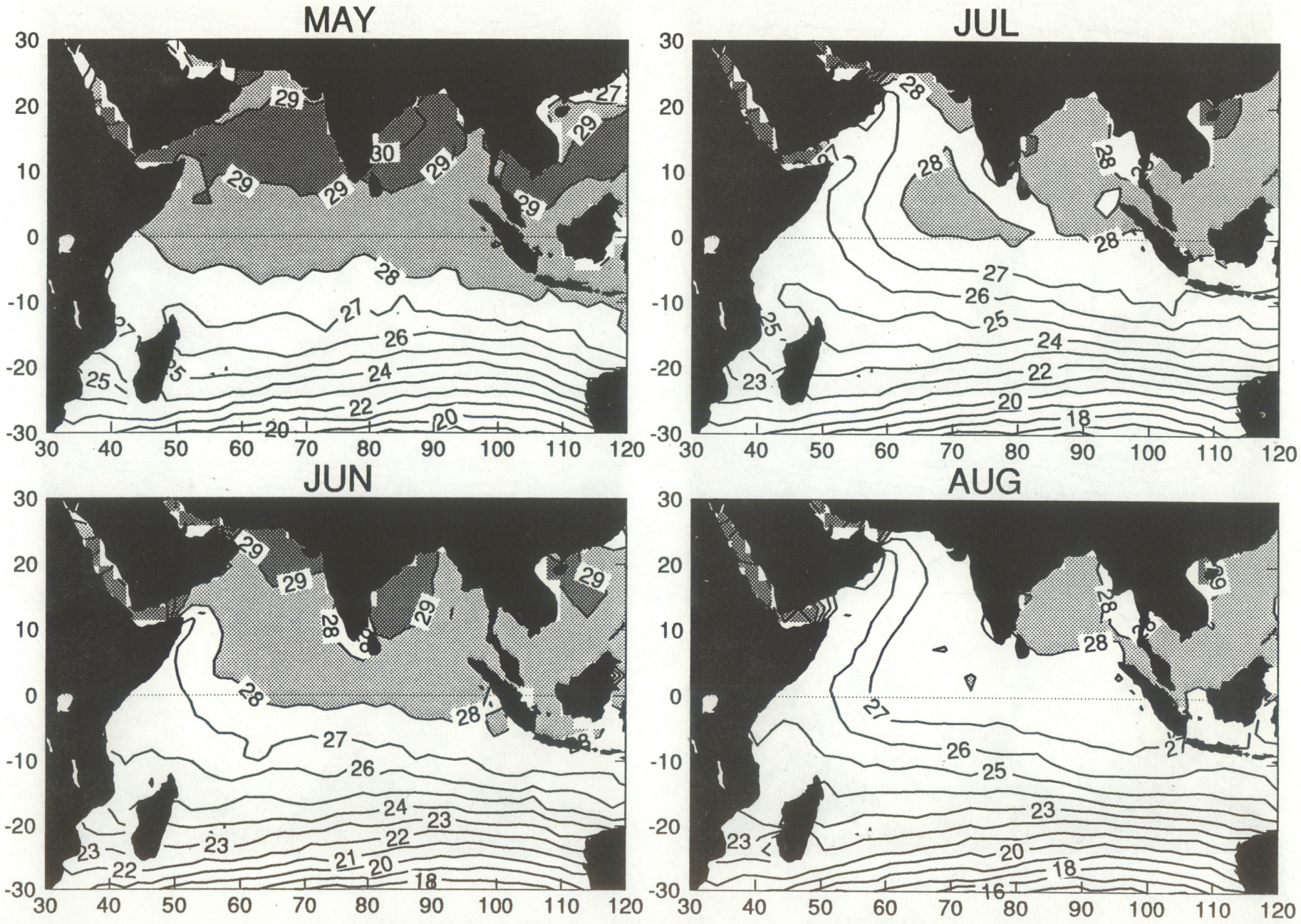

Figure 9

MEAN AIR TEMP(c) FIELDS

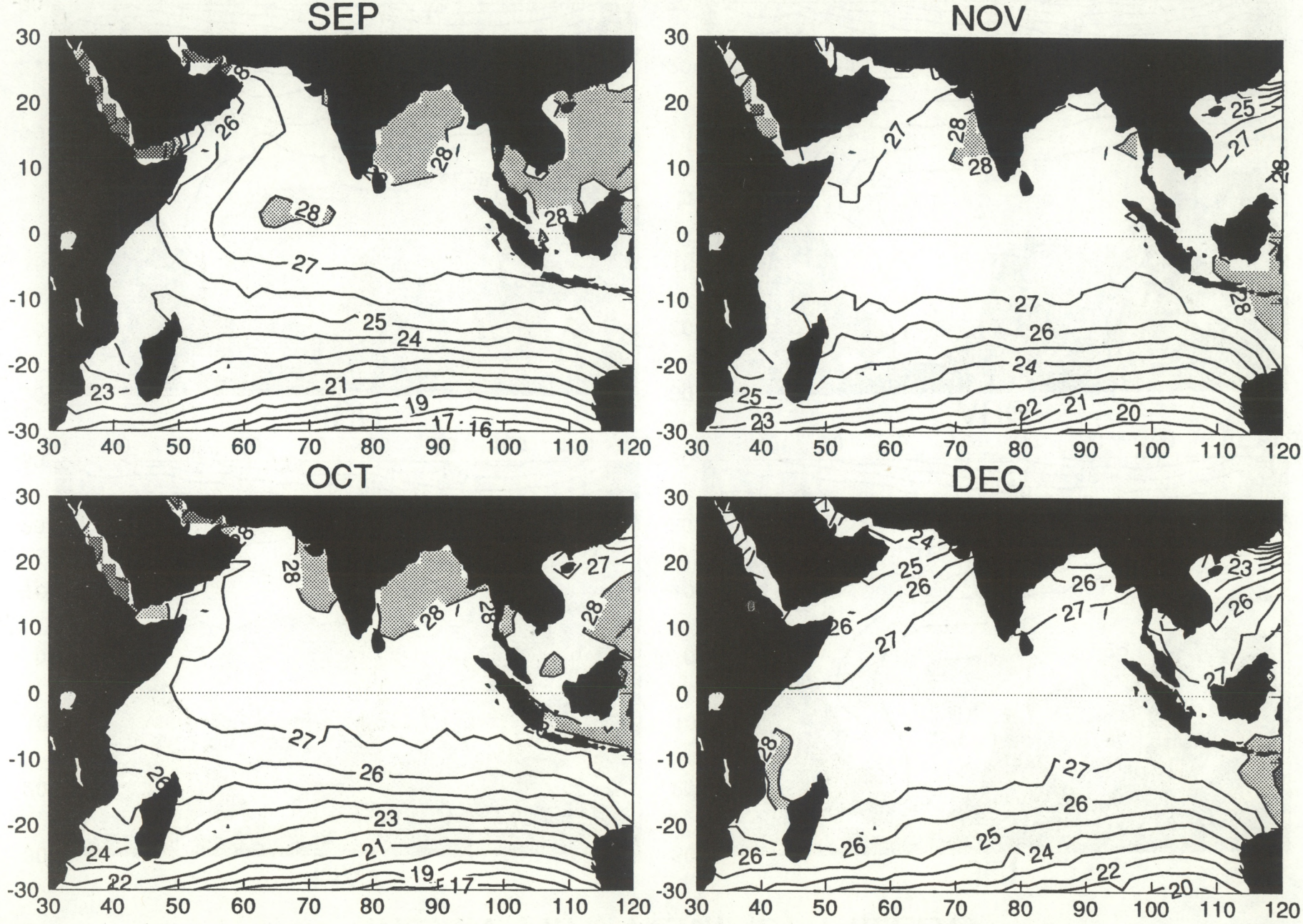

Figure 10

MEAN SPECIFIC HUMIDITY(gm/kg) FIELDS

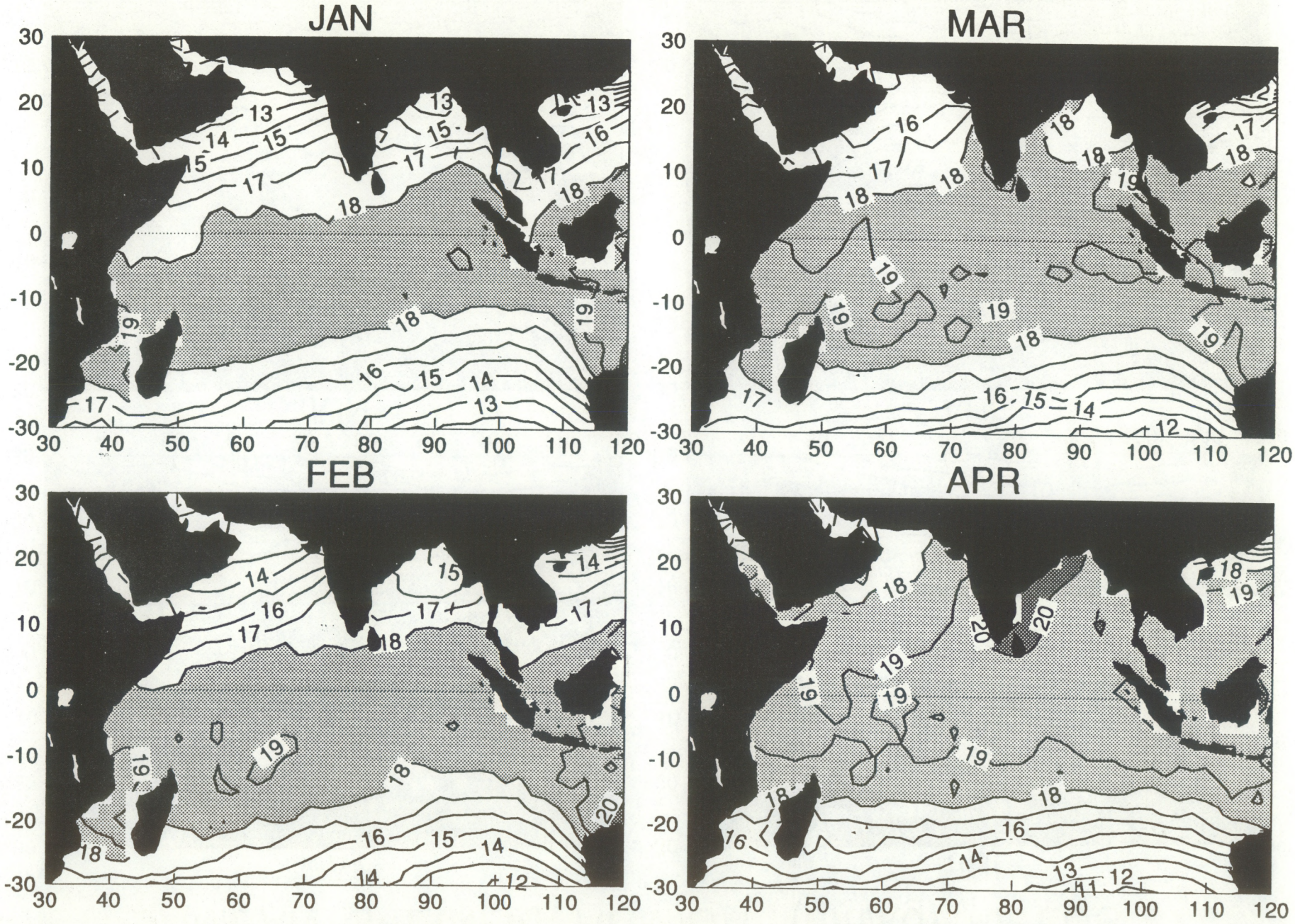

Figure 11

MEAN SPECIFIC HUMIDITY(gm/kg) FIELDS

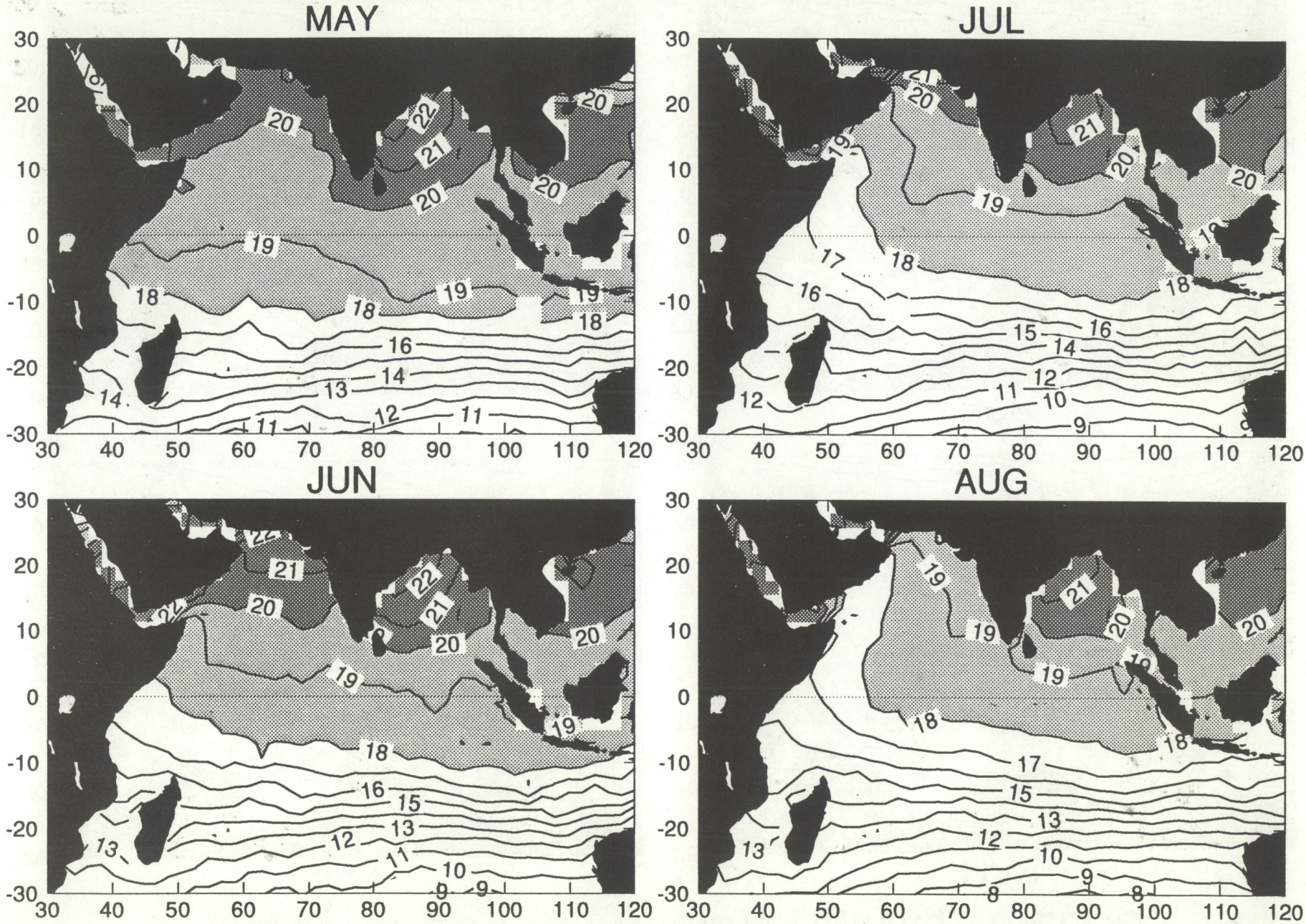

Figure 12

MEAN SPECIFIC HUMIDITY(gm/kg) FIELDS

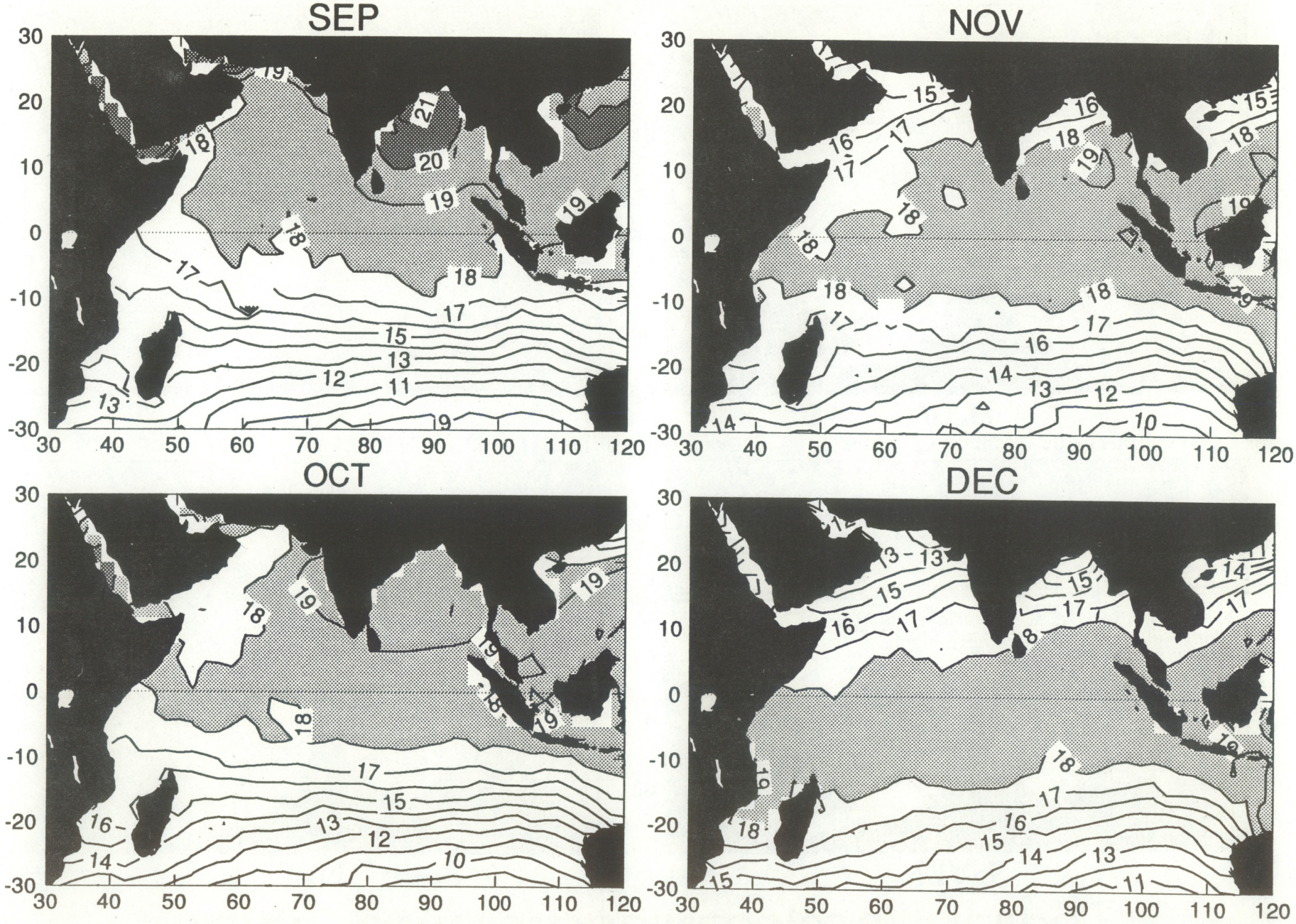

Figure 13

MEAN TOTAL CLOUDINESS(octa) FIELDS

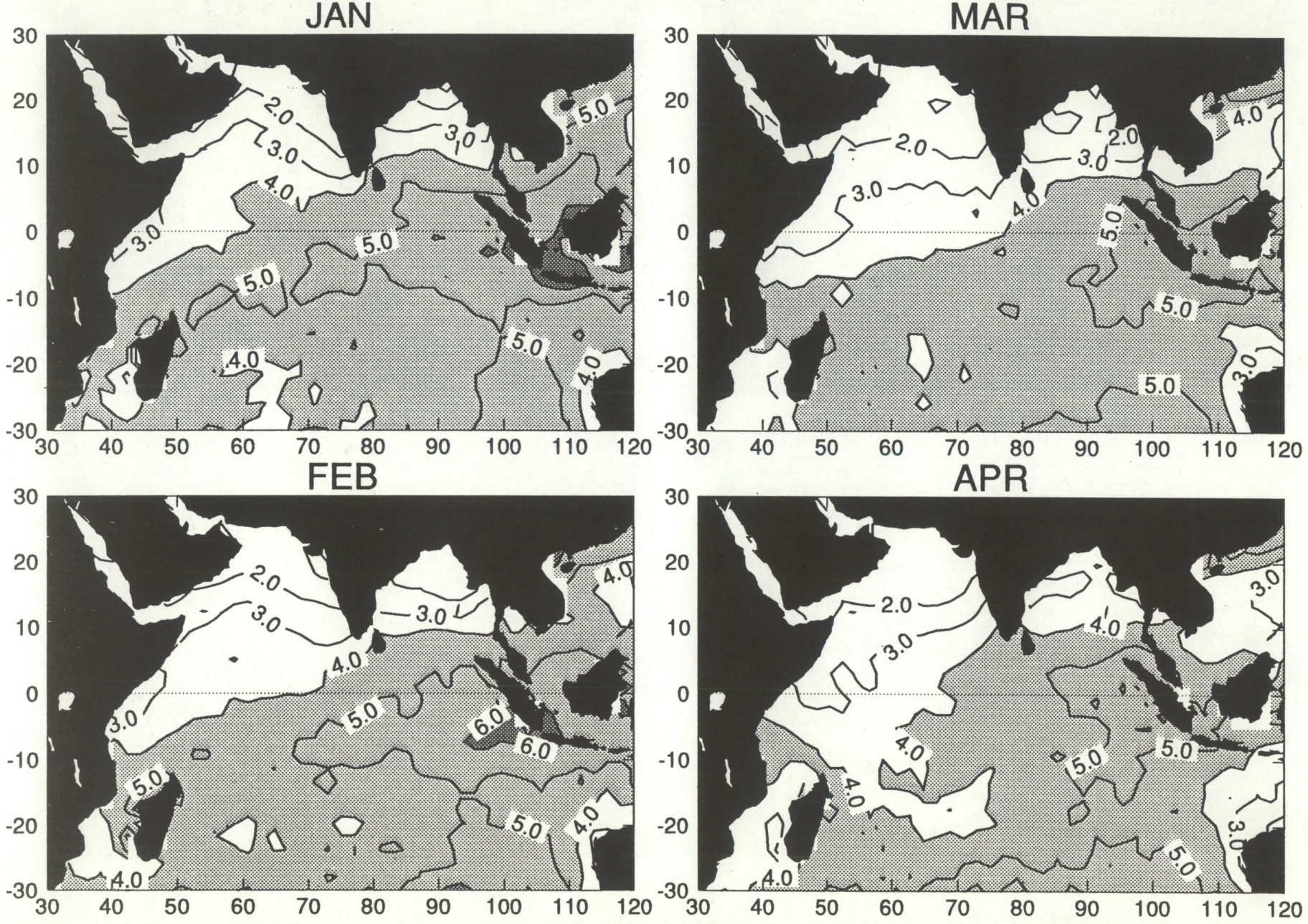

Figure 14

MEAN TOTAL CLOUDINESS(octa) FIELDS

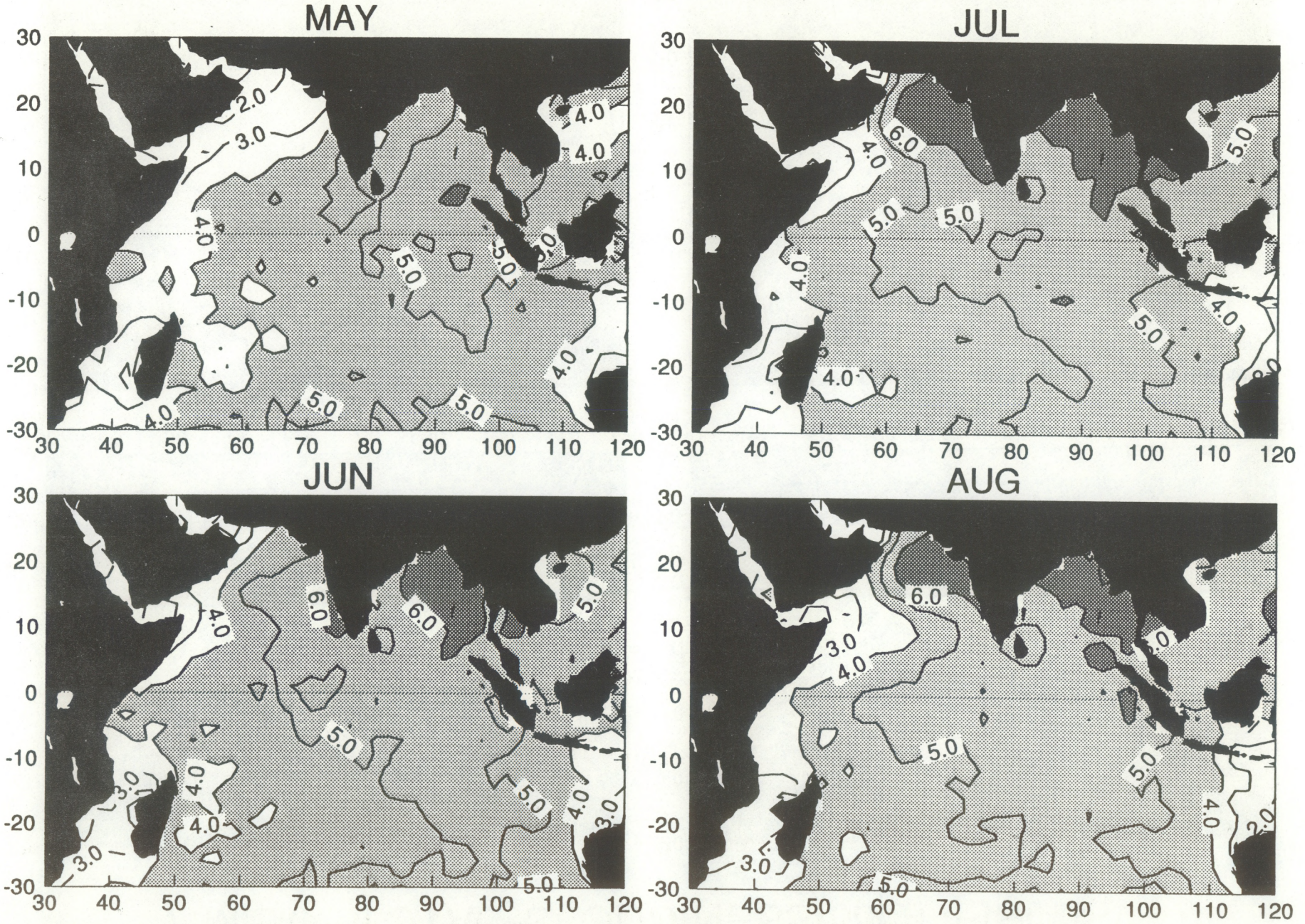

Figure 15

MEAN TOTAL CLOUDINESS(octa) FIELDS

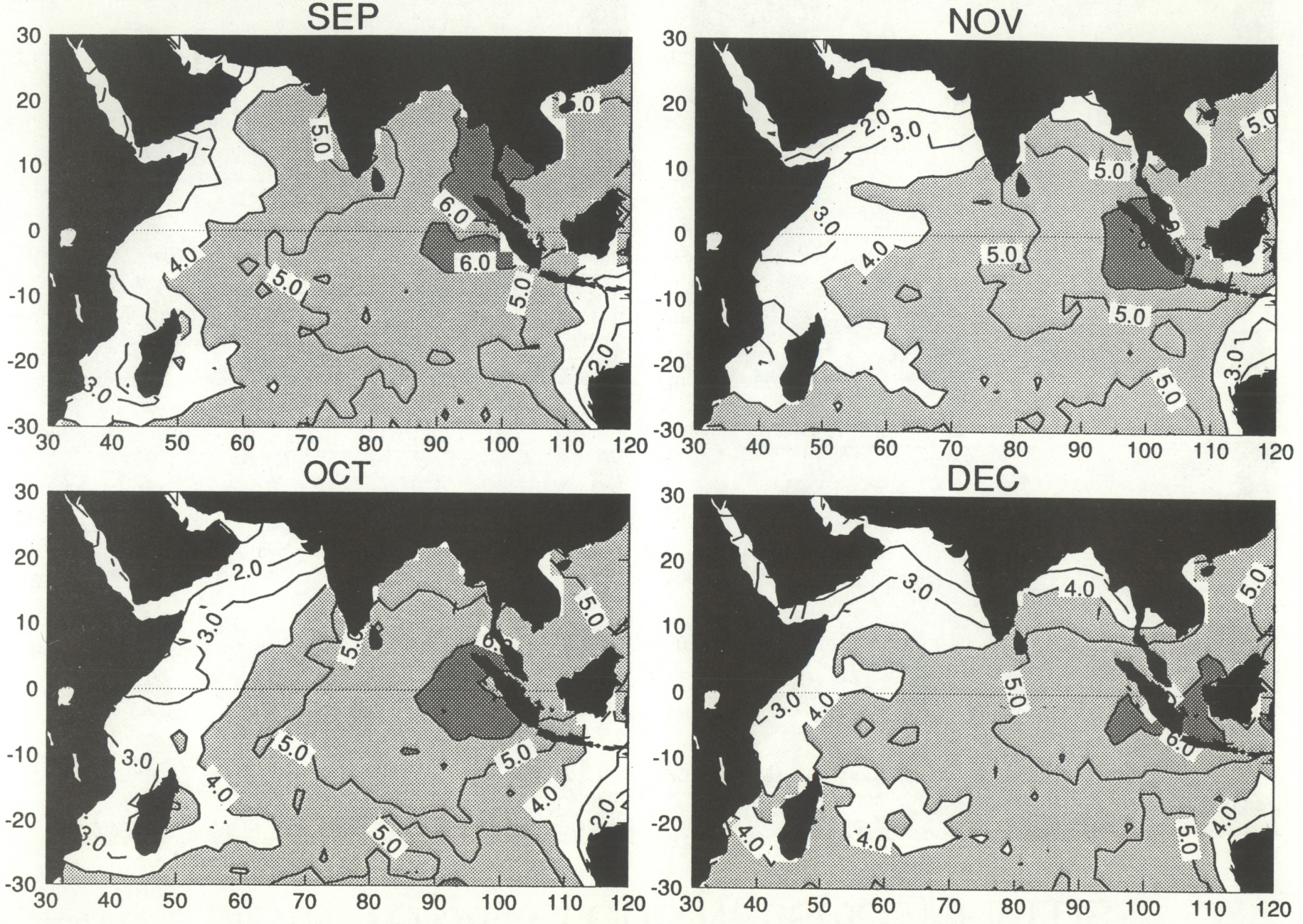

Figure 16

OBSERVED MEAN SST(c) FIELDS

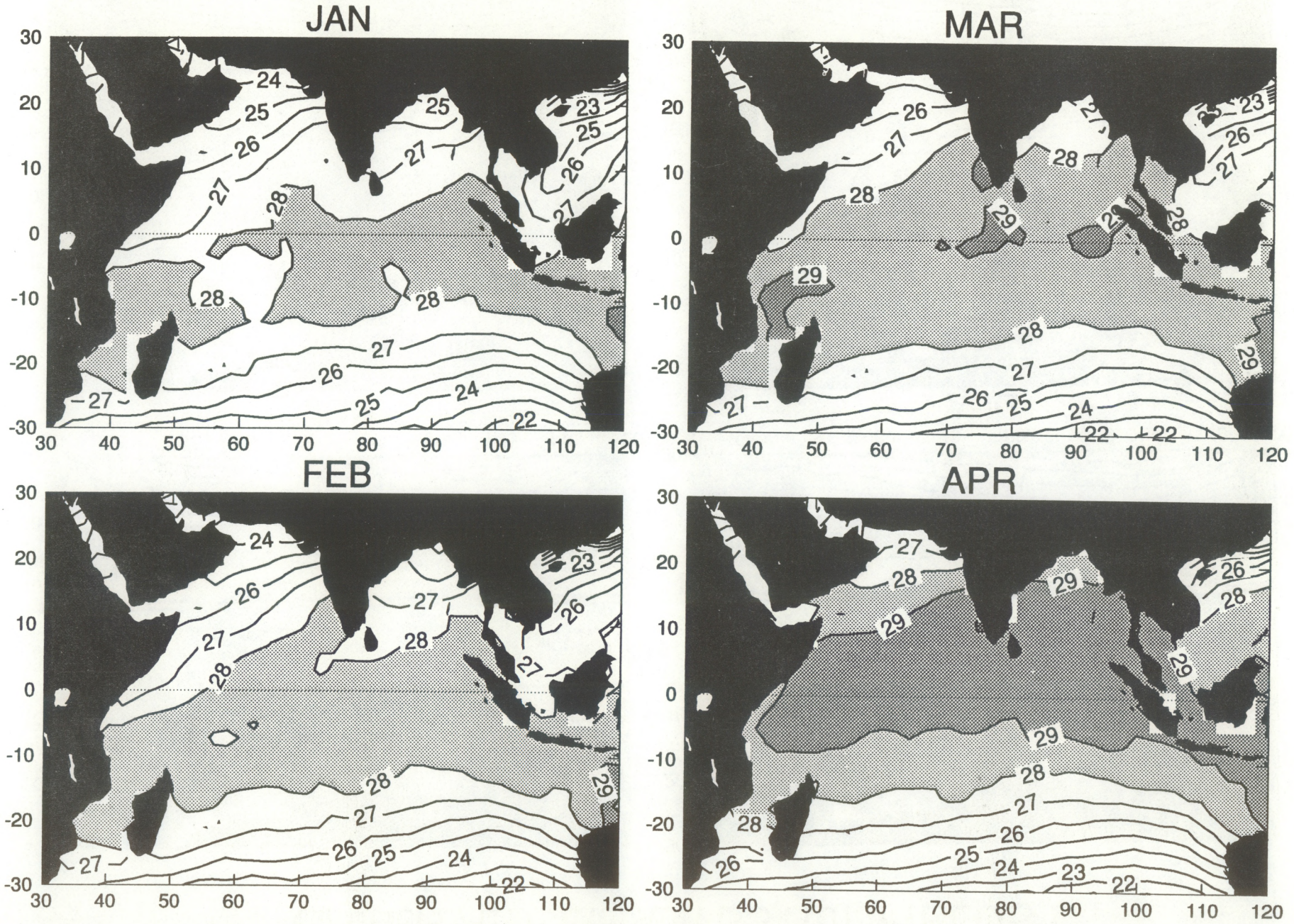

Figure 17

OBSERVED MEAN SST(c) FIELDS

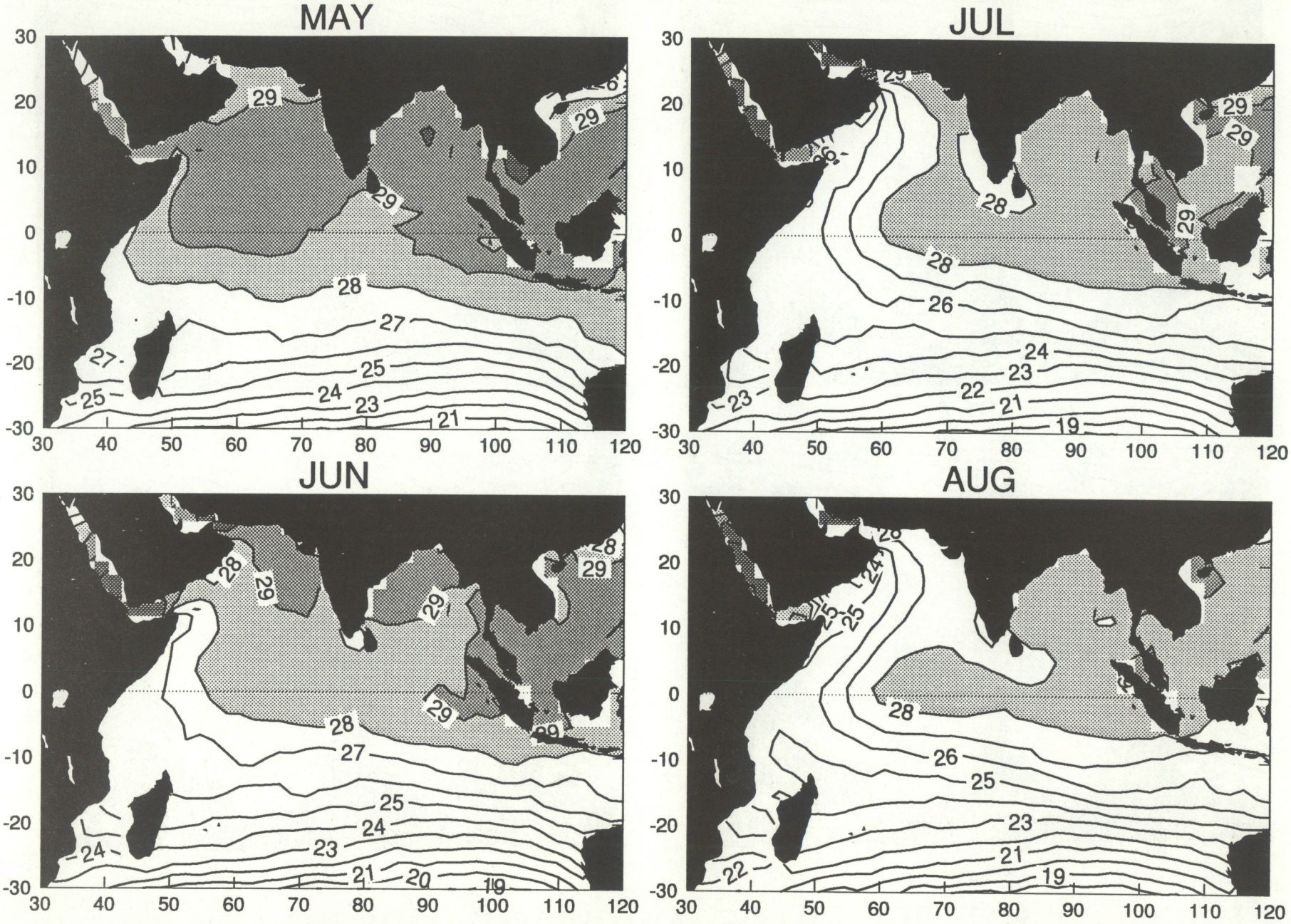

Figure 18

OBSERVED MEAN SST(c) FIELDS

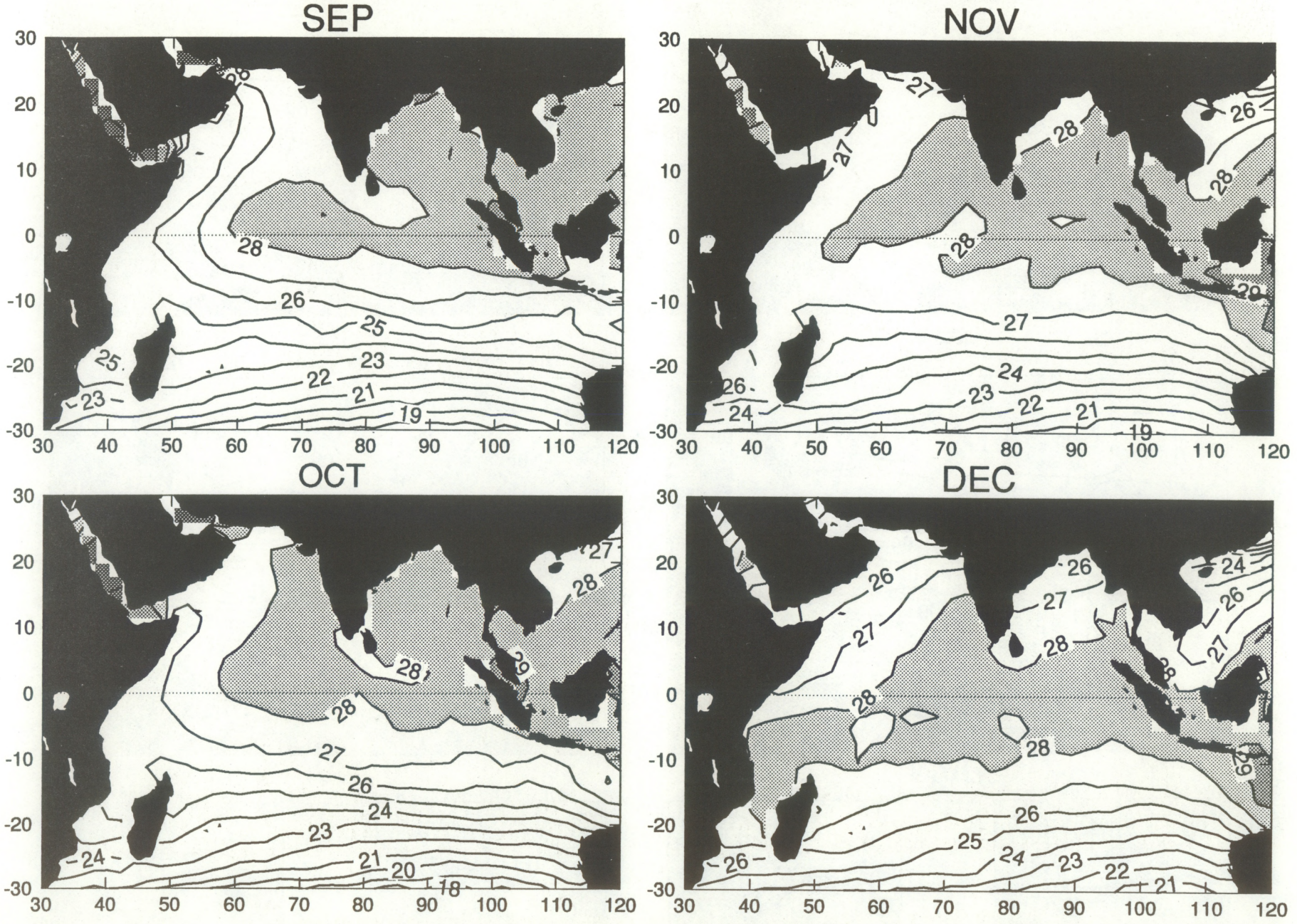

Figure 19

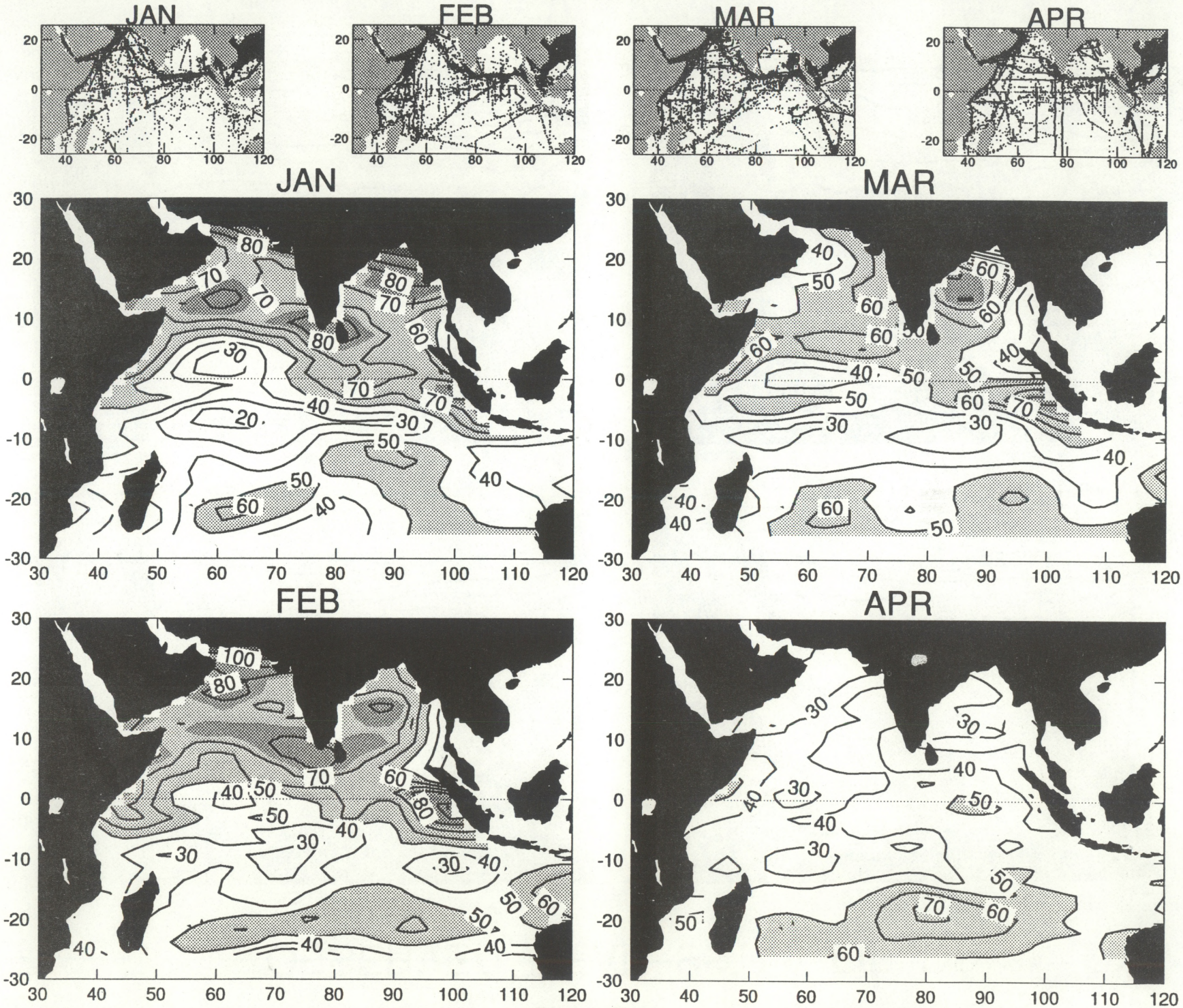

Figure 20

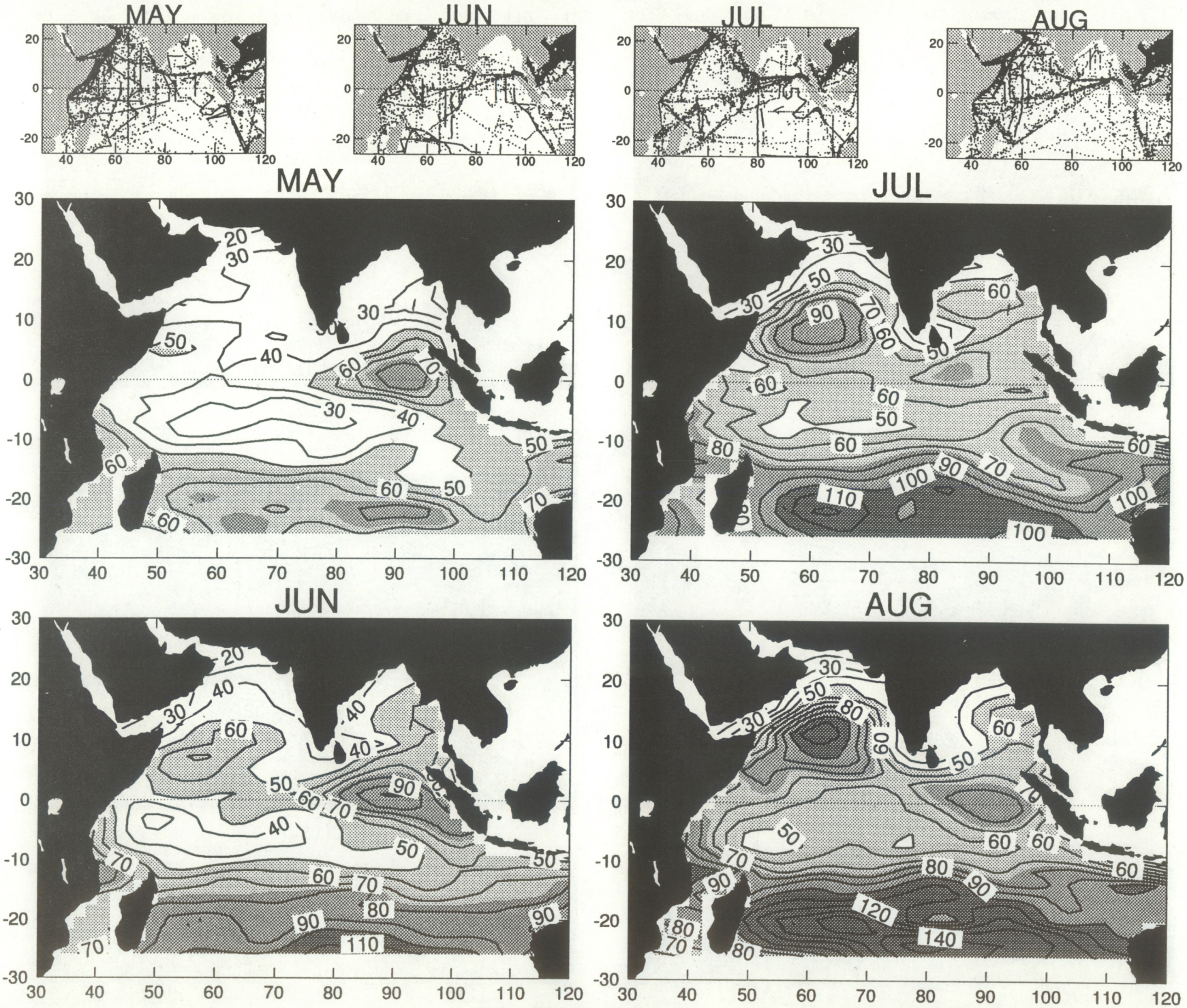

Figure 21

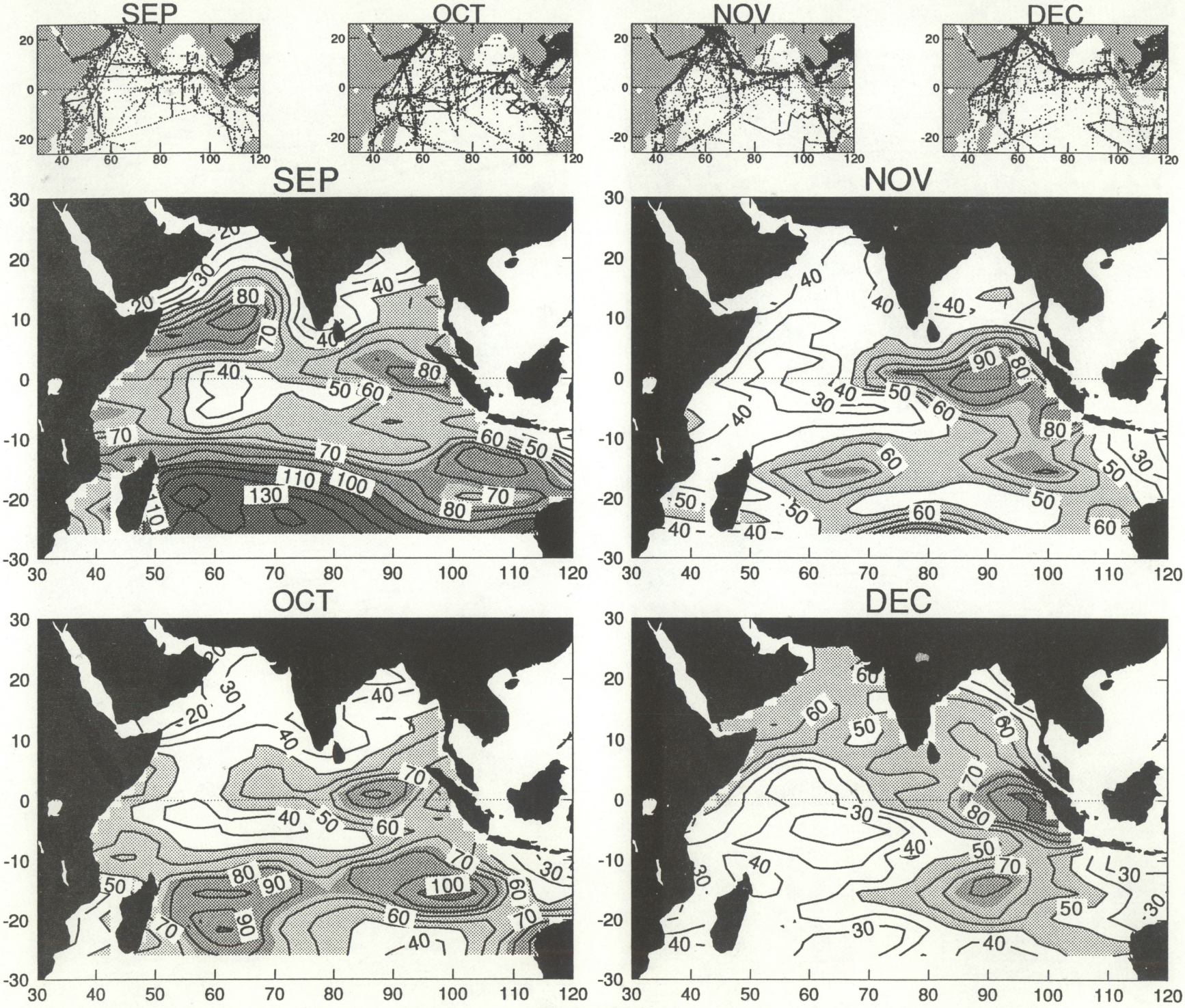

Figure 22

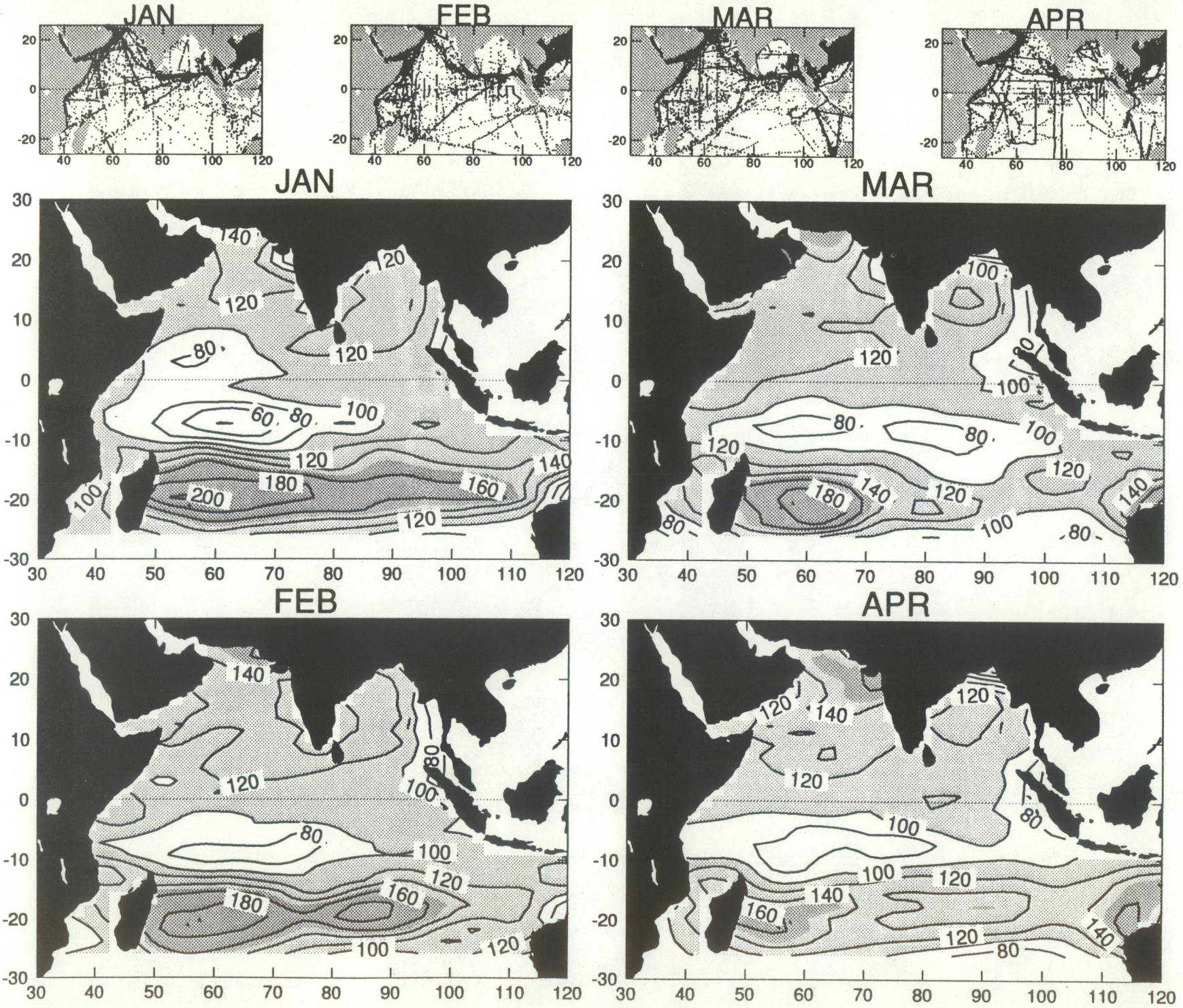

Figure 23

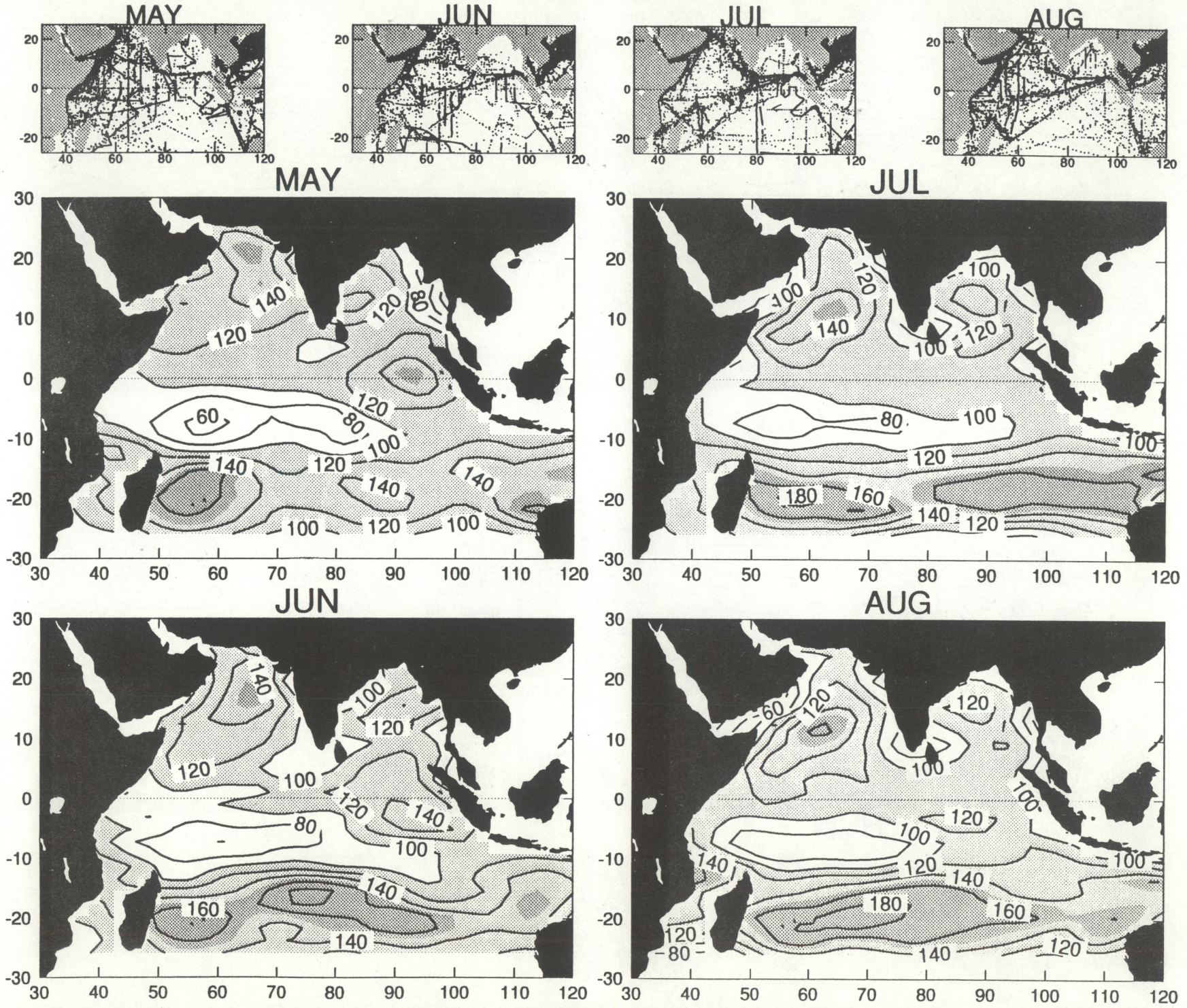

Figure 24

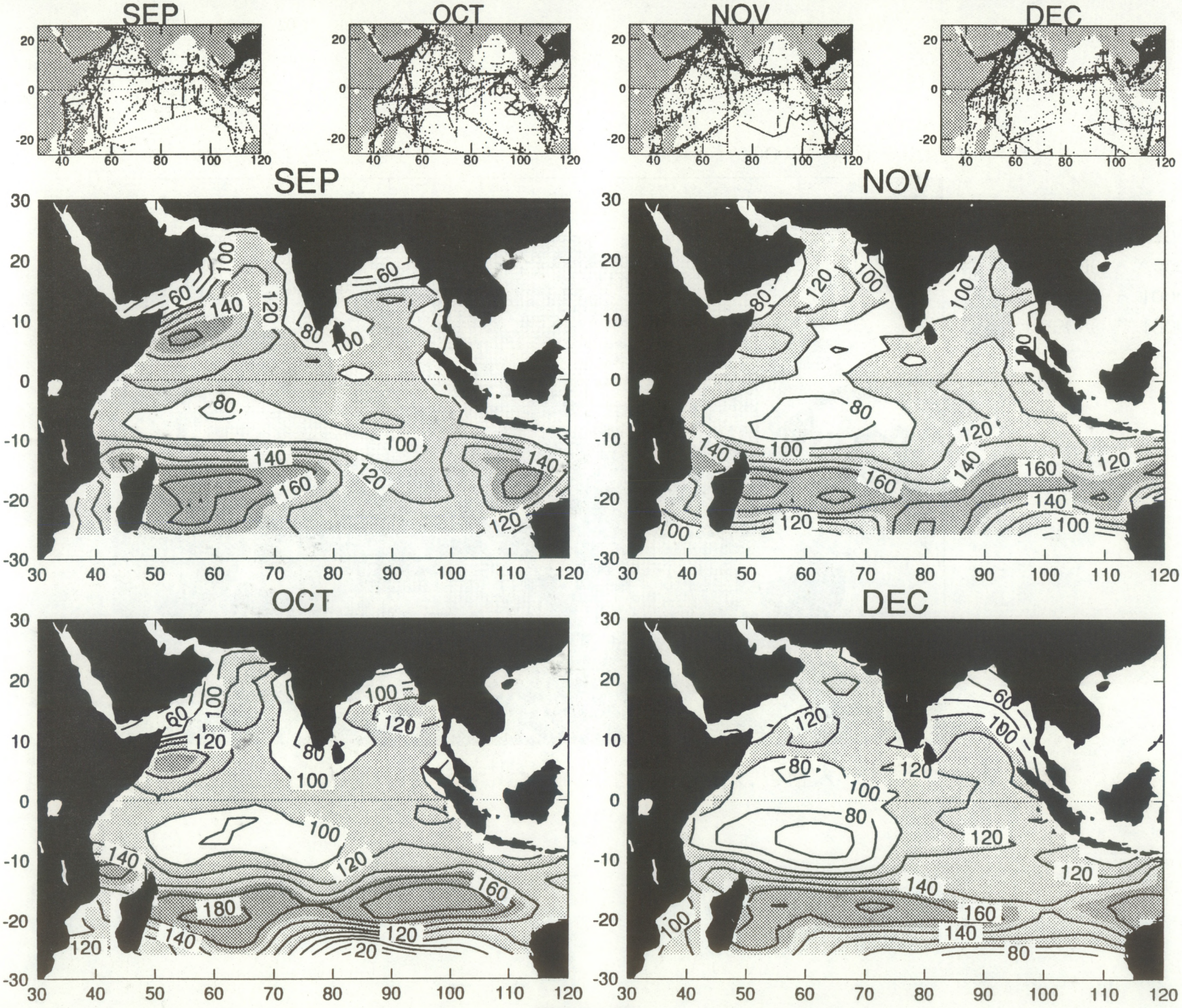

Figure 25

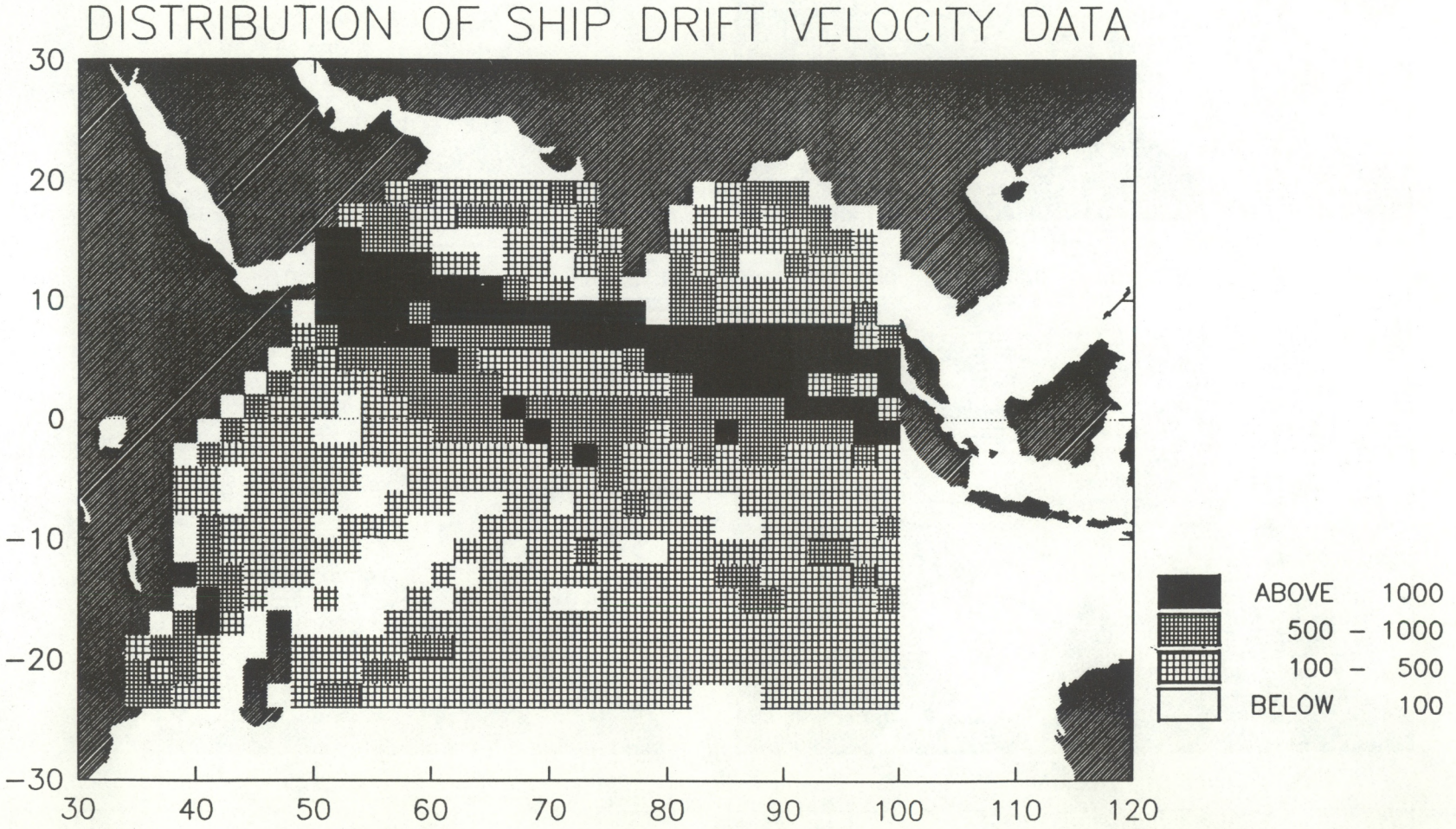
DISTRIBUTION OF SHIP DRIFT VELOCITY DATA
30
20
10
0
−10
−20
−30
30
40
50
60
70
80
90
100
110
120
ABOVE 1000
500 – 1000
100 – 500
BELOW 100

Figure 26

OBSERVED SHIP DRIFT CURRENT VECTORS

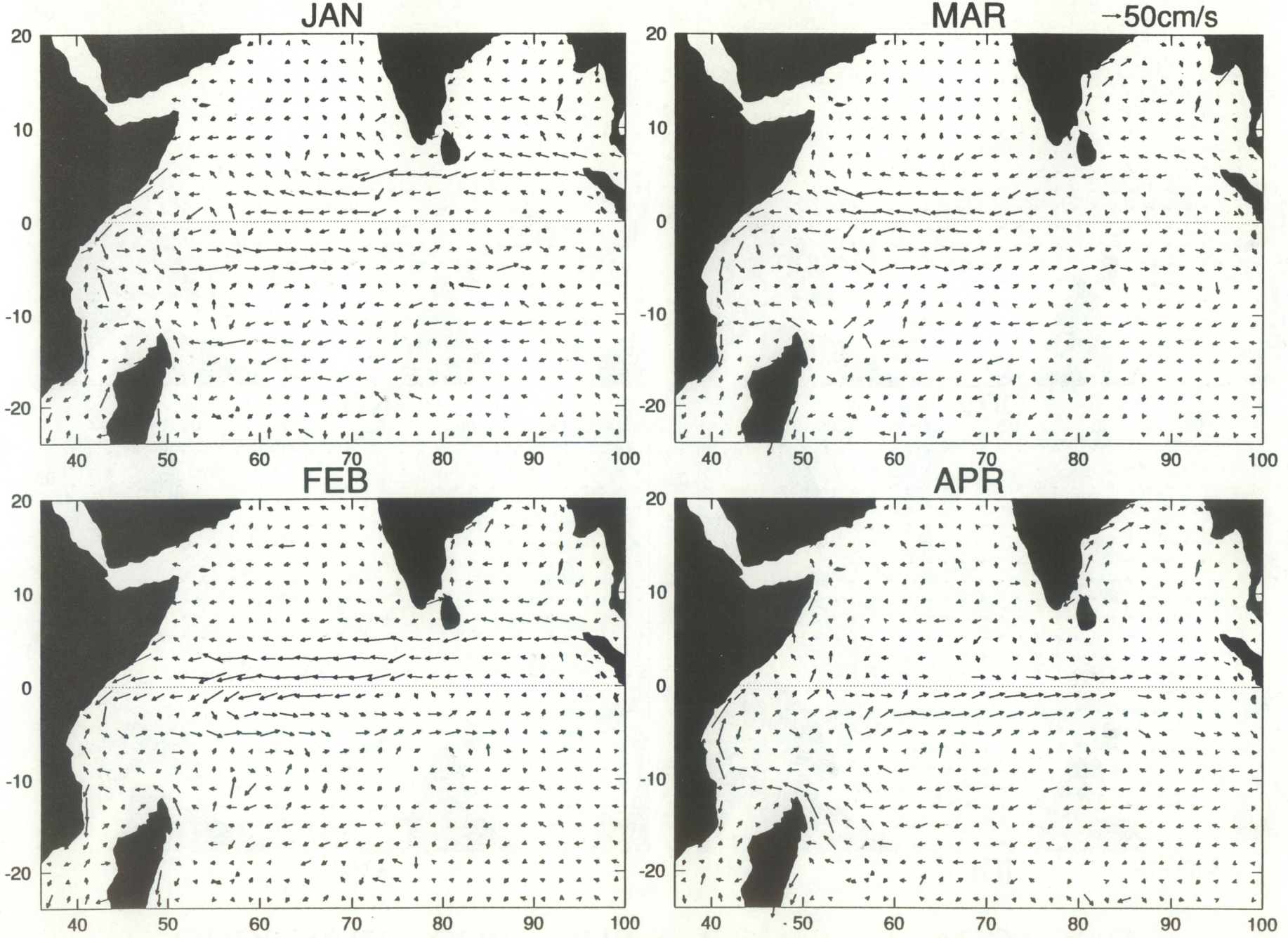

Figure 27

OBSERVED SHIP DRIFT CURRENT VECTORS

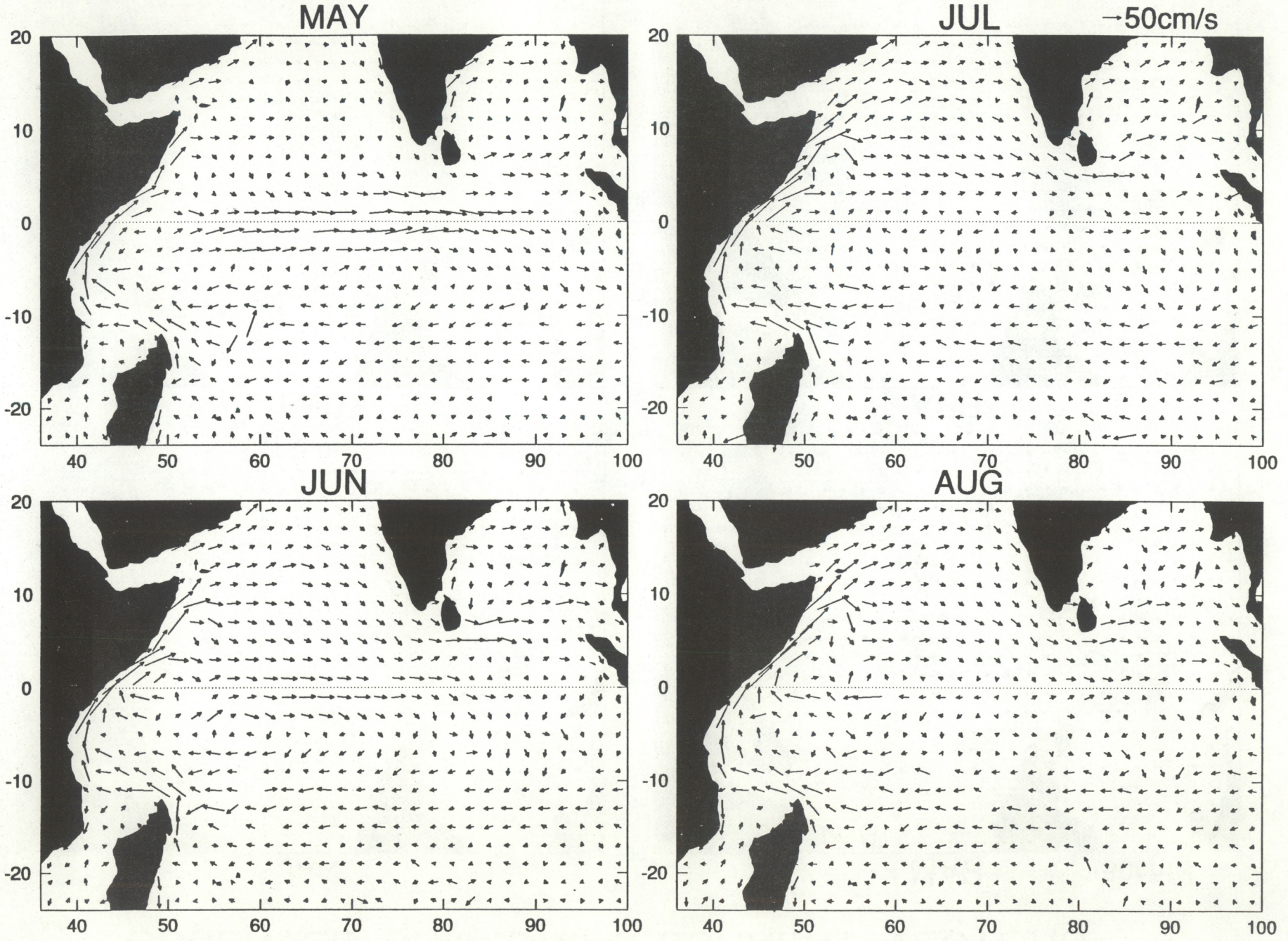

Figure 28

OBSERVED SHIP DRIFT CURRENT VECTORS

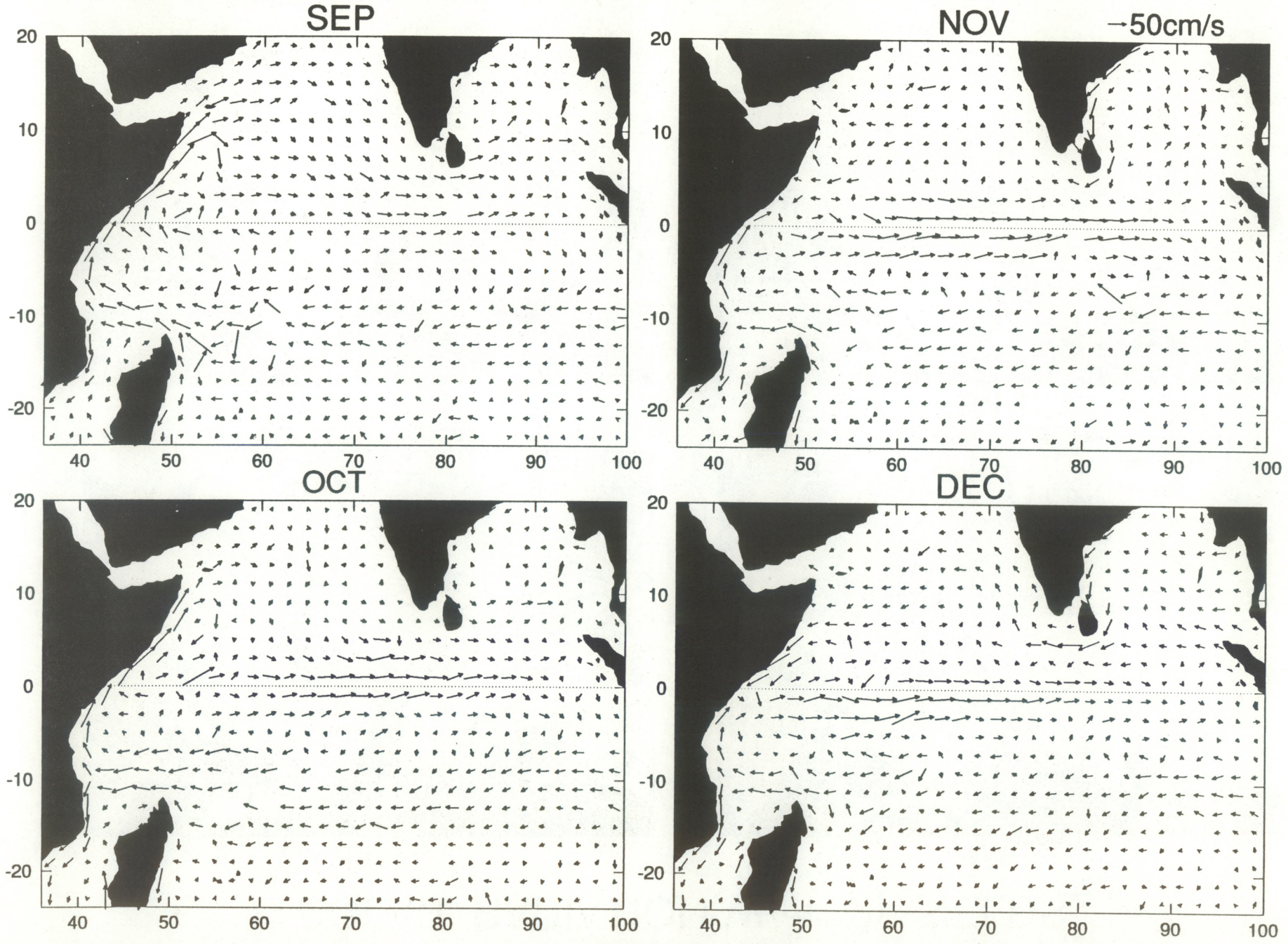

Figure 29

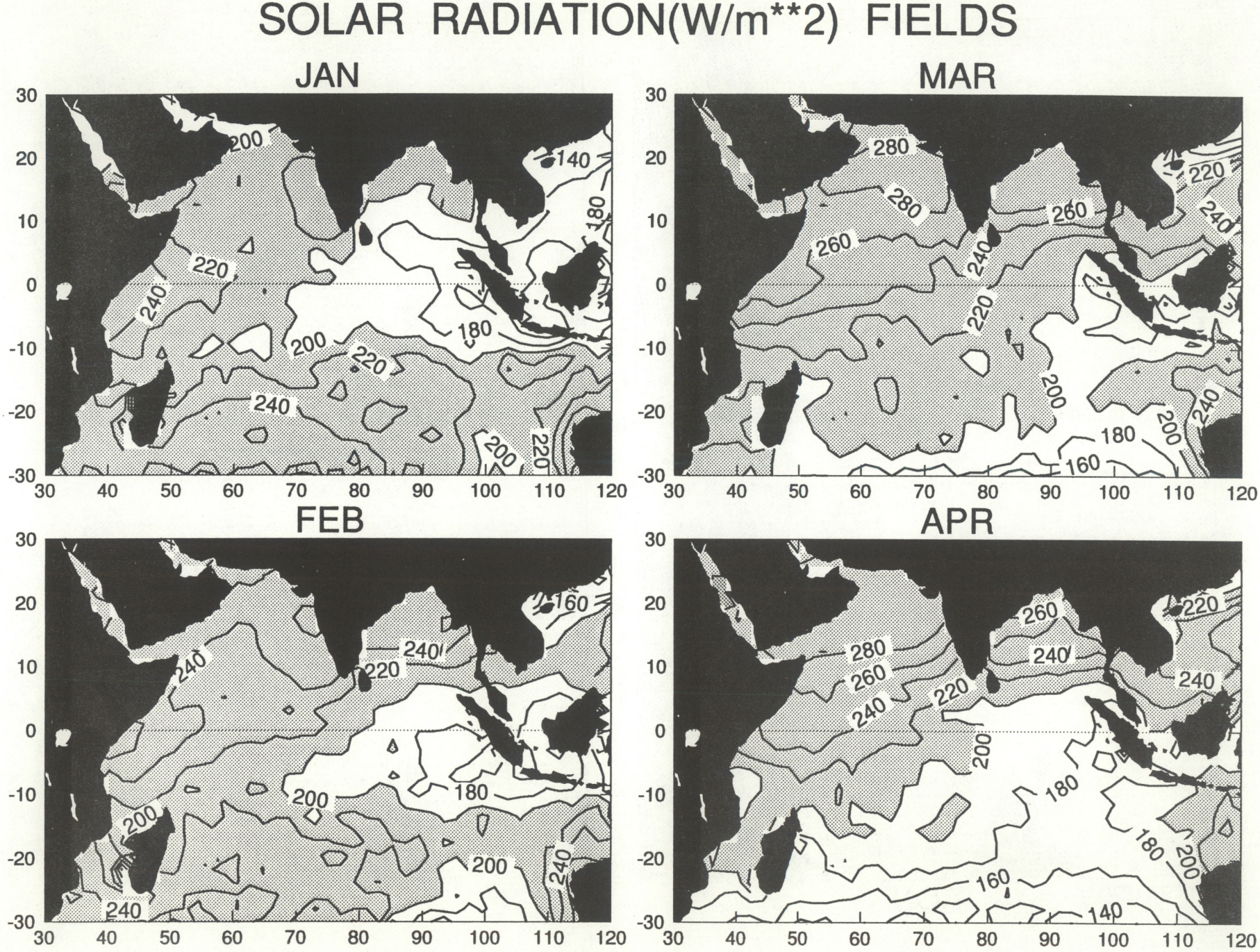
SOLAR RADIATION(W/m**2) FIELDS
JAN
MAR
FEB
APR
30
20
10
0
-10
-20
-30
30 40 50 60 70 80 90 100 110 120
200
140
180
220
240
280
260
160

Figure 30

SOLAR RADIATION(W/m**2) FIELDS

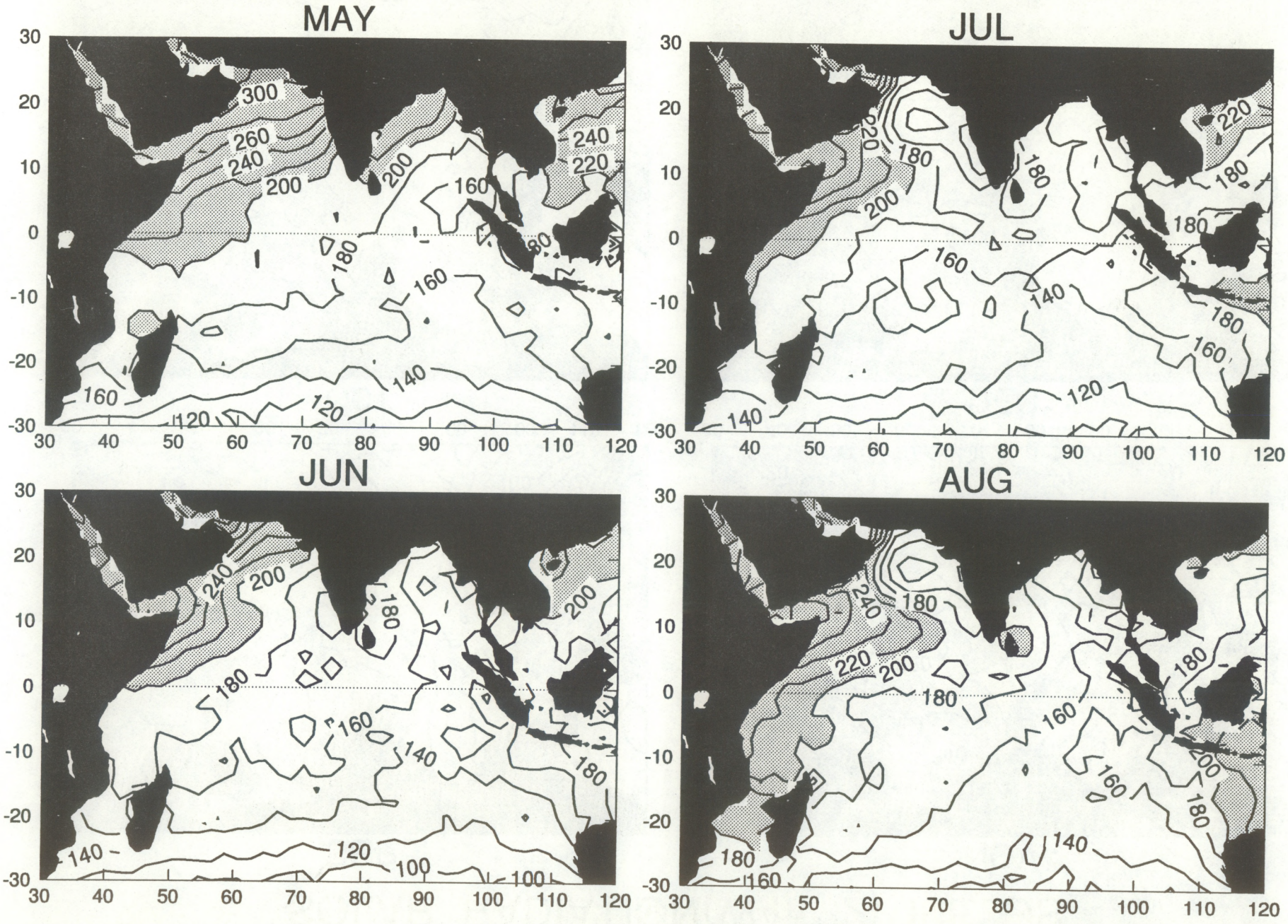

Figure 31

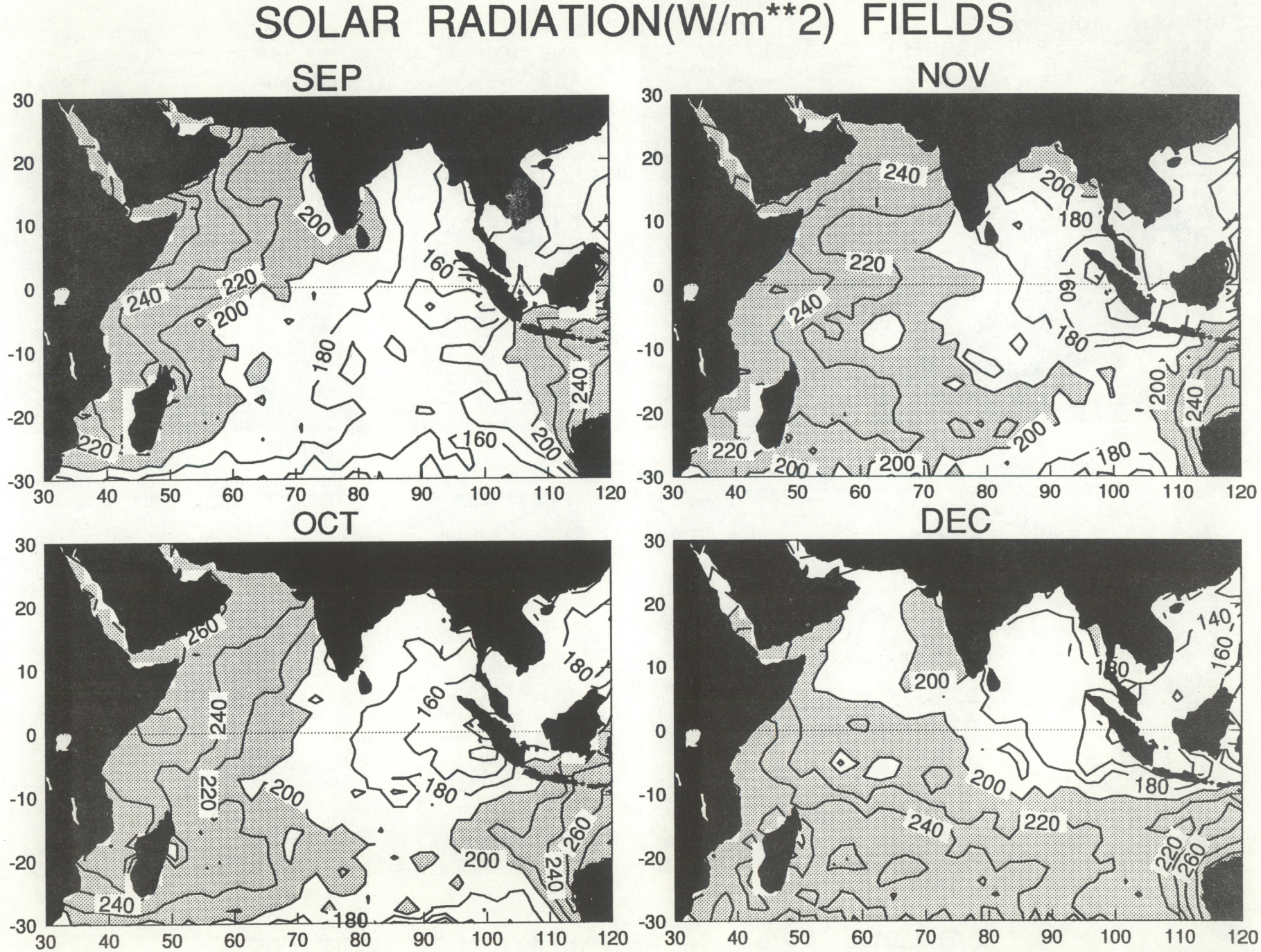

Figure 32

NET LONGWAVE RADIATION(W/m**2) FIELDS

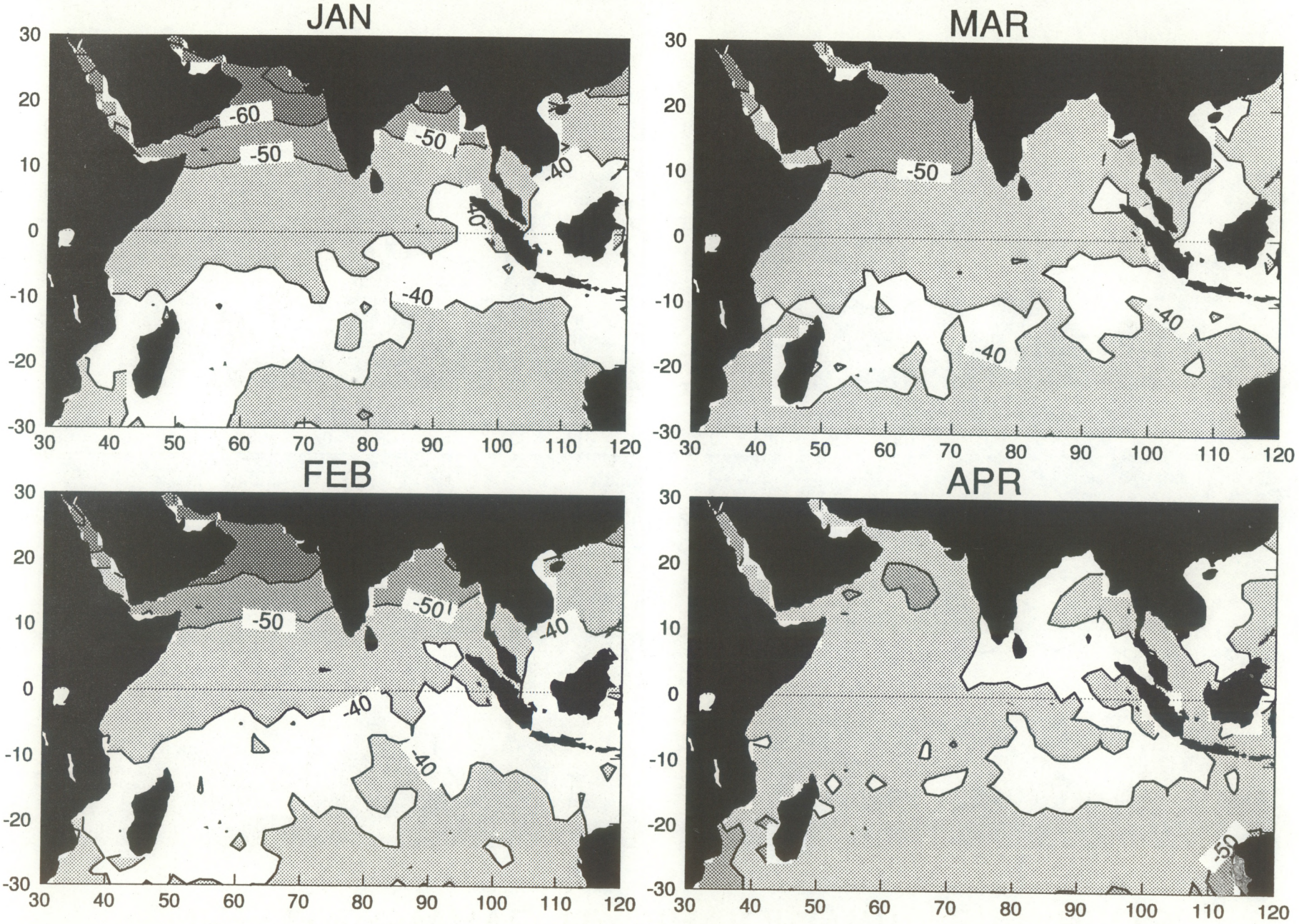

Figure 33

NET LONGWAVE RADIATION(W/m**2) FIELDS

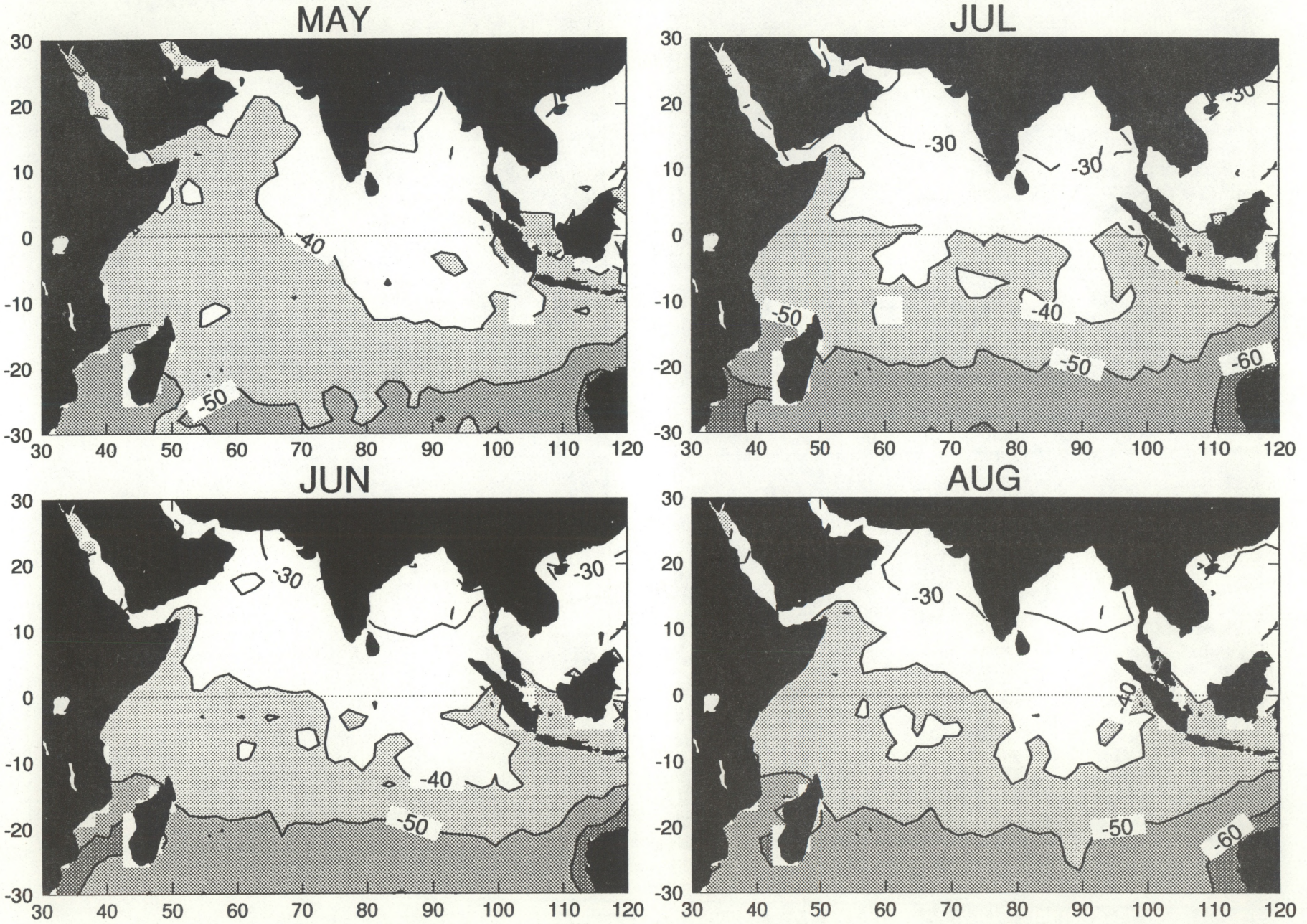

Figure 34

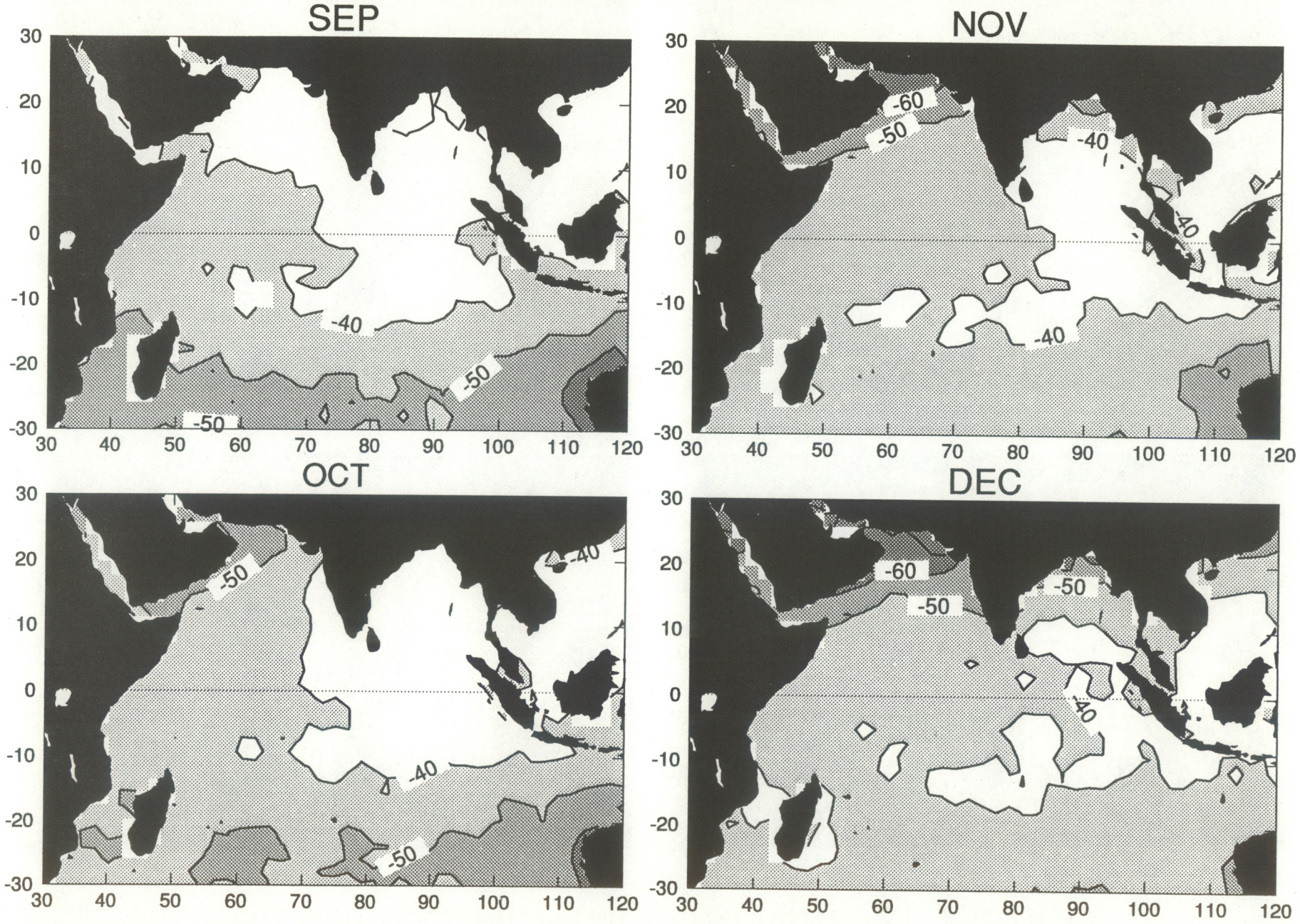
NET LONGWAVE RADIATION(W/m**2) FIELDS
SEP
NOV
OCT
DEC
-40
-50
-60
30
20
10
0
-10
-20
-30
30
40
50
60
70
80
90
100
110
120

Figure 35

SENSIBLE HEAT FLUX(W/m**2) FIELDS

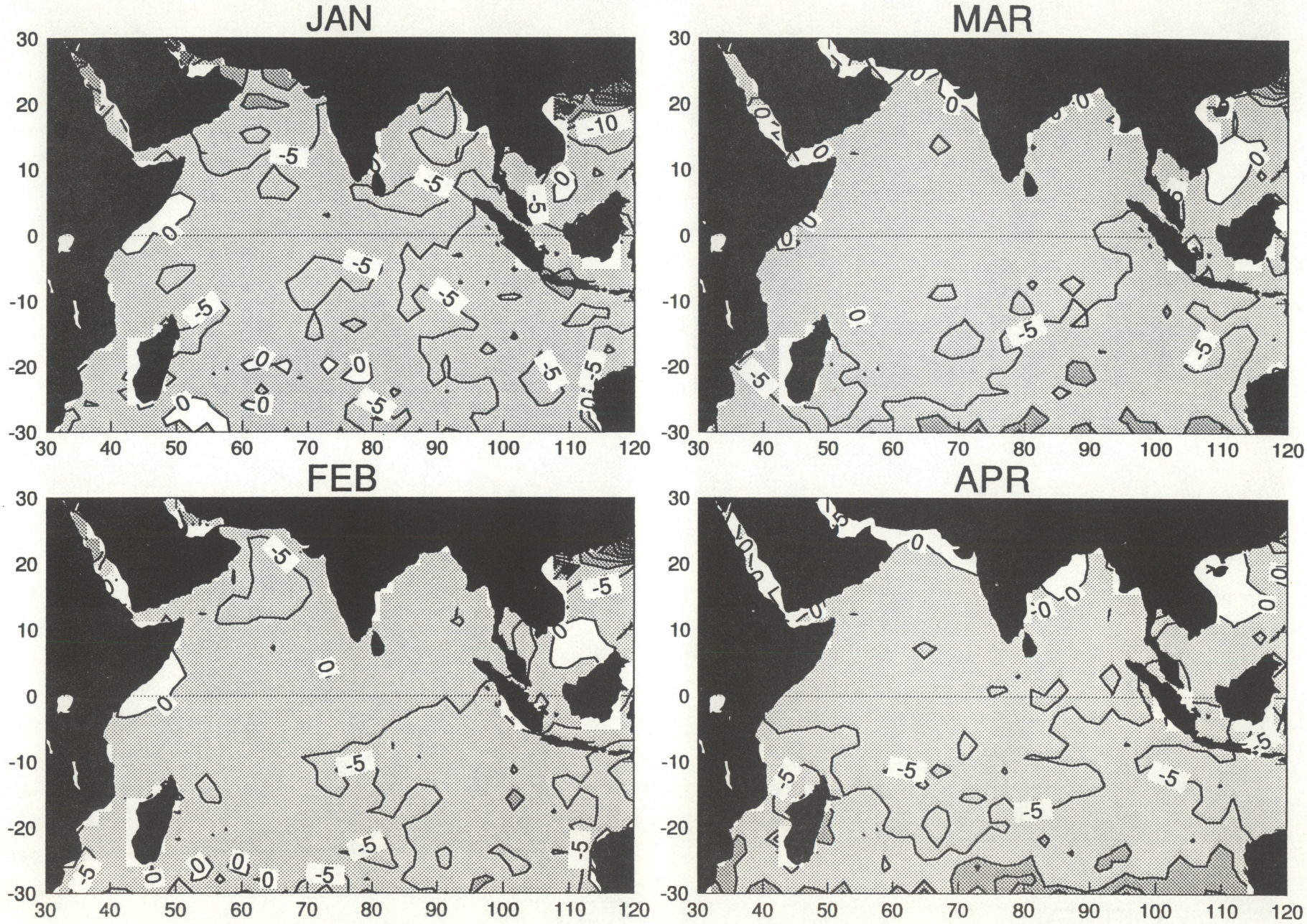

Figure 36

SENSIBLE HEAT FLUX(W/m**2) FIELDS

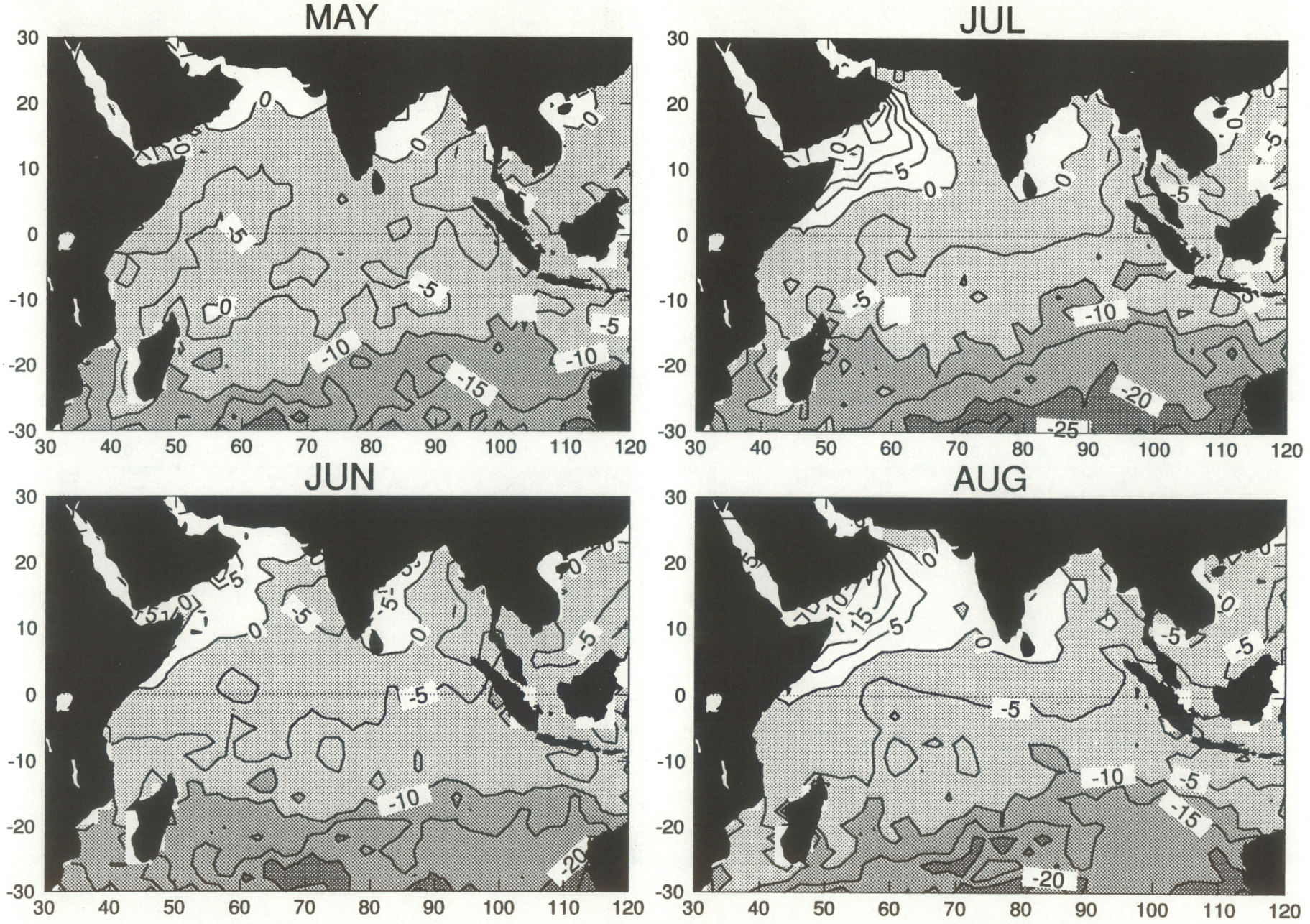

Figure 37

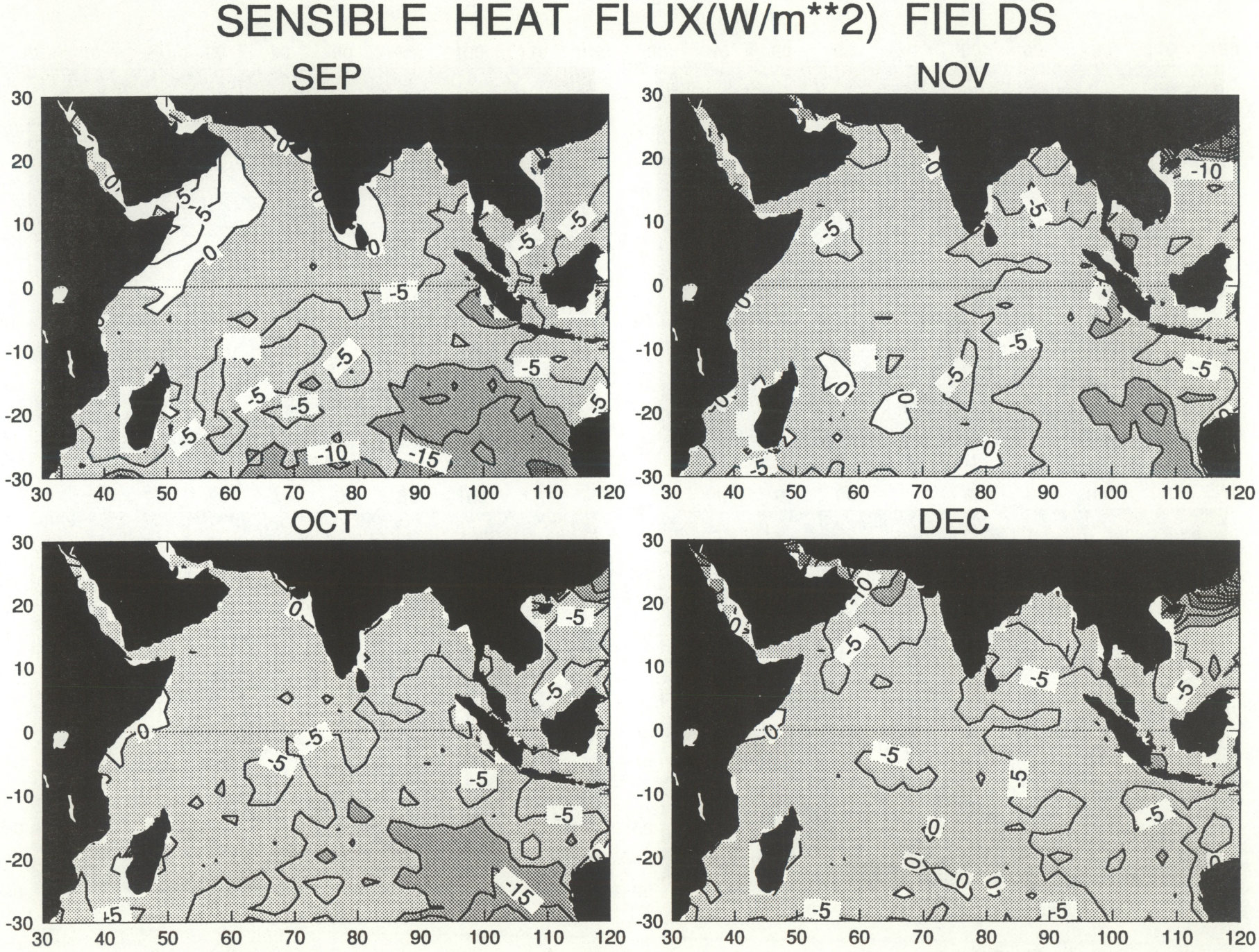

Figure 38

LATENT HEAT FLUX(W/m**2) FIELDS

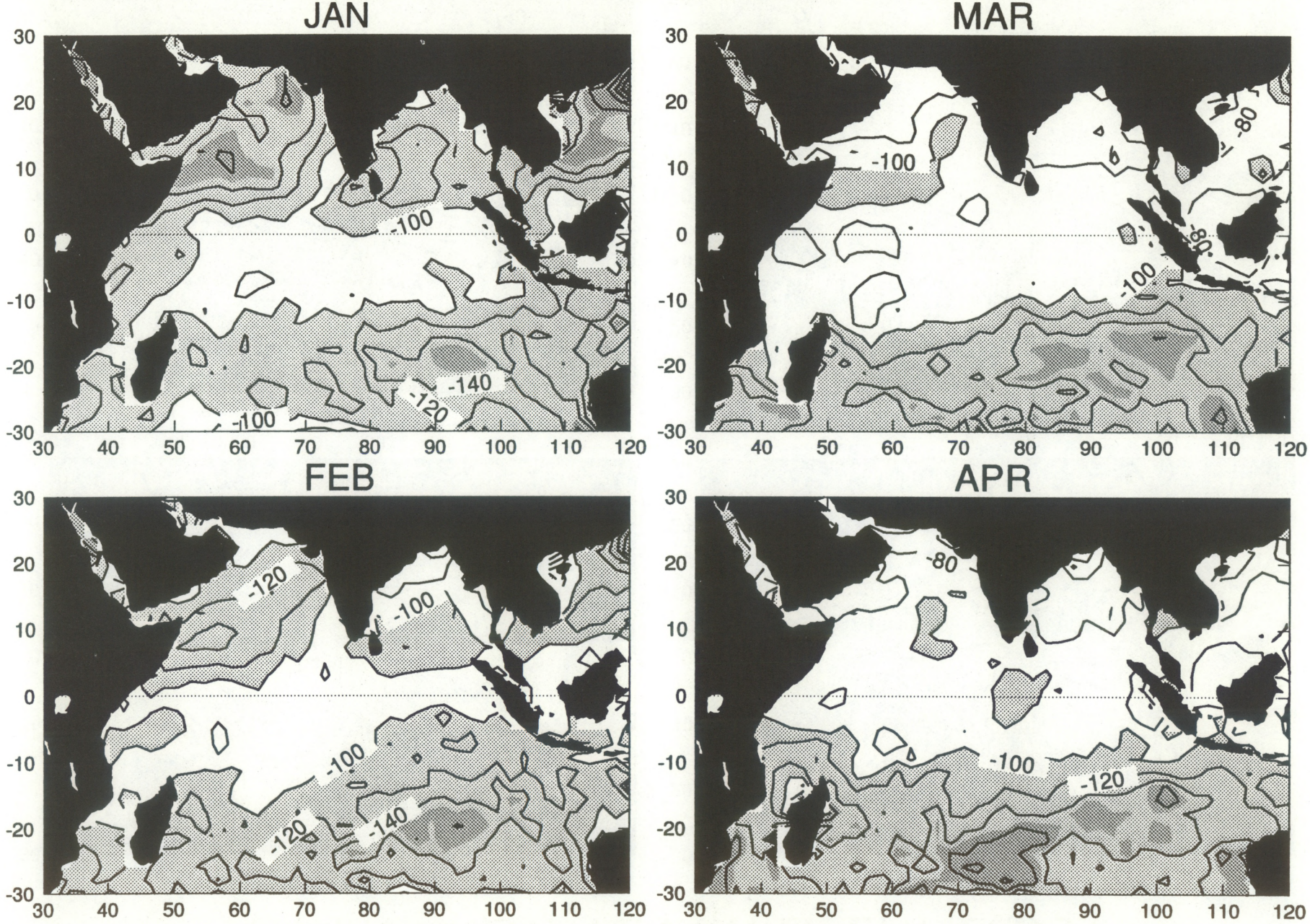

Figure 39

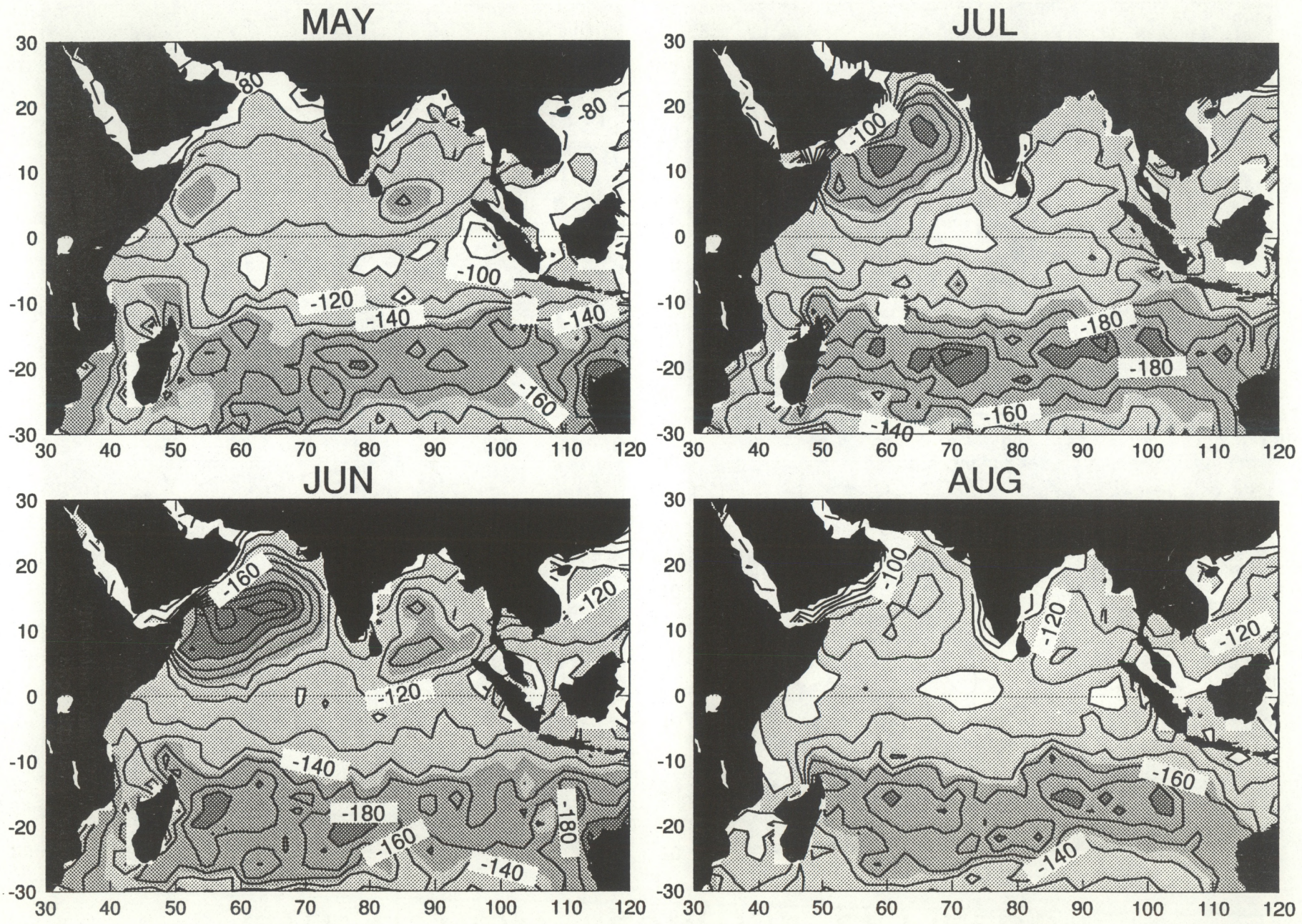
LATENT HEAT FLUX(W/m**2) FIELDS
MAY
JUL
JUN
AUG
30
20
10
0
-10
-20
-30
30 40 50 60 70 80 90 100 110 120
-80
-100
-120
-140
-160
-180

Figure 40

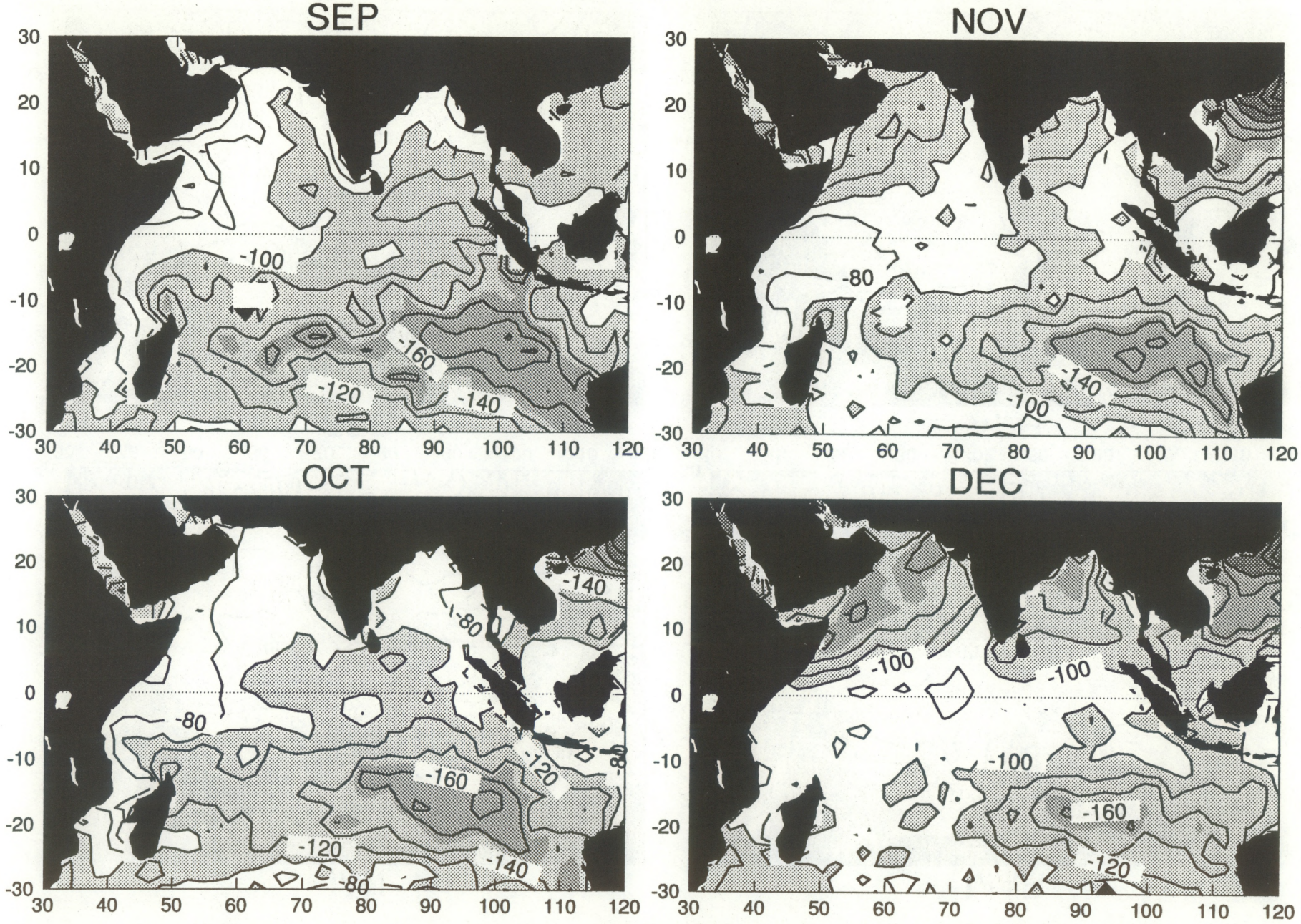
LATENT HEAT FLUX(W/m**2) FIELDS
SEP
NOV
OCT
DEC
-100
-160
-120
-140
-80
-140
-100
-80
-140
-80
-160
-120
-80
-120
-140
-80
-100
-100
-100
-160
-120
30
20
10
0
-10
-20
-30
30
40
50
60
70
80
90
100
110
120

Figure 41

SURFACE NET HEAT FLUX(W/m**2) FIELDS

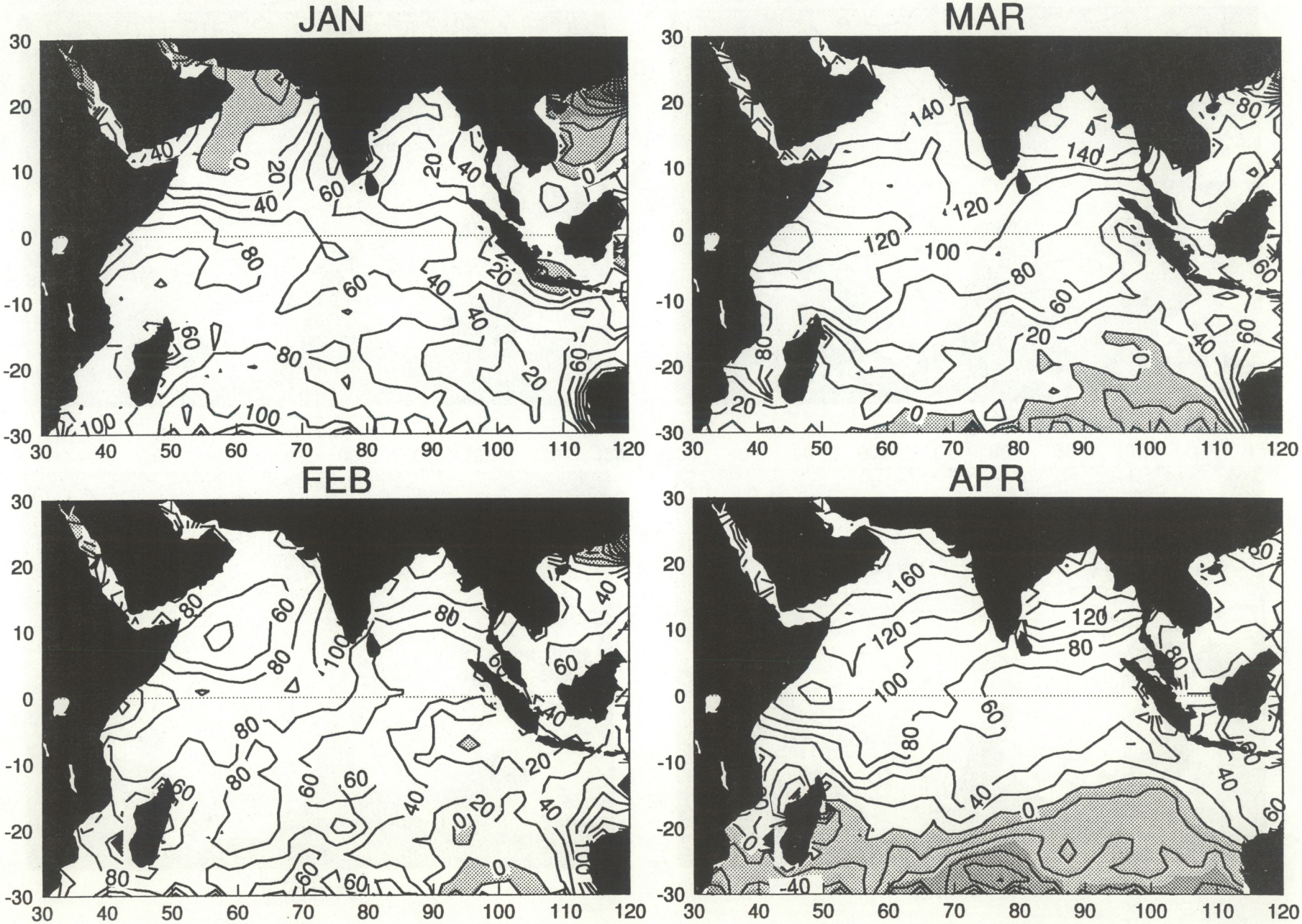

Figure 42

SURFACE NET HEAT FLUX(W/m**2) FIELDS

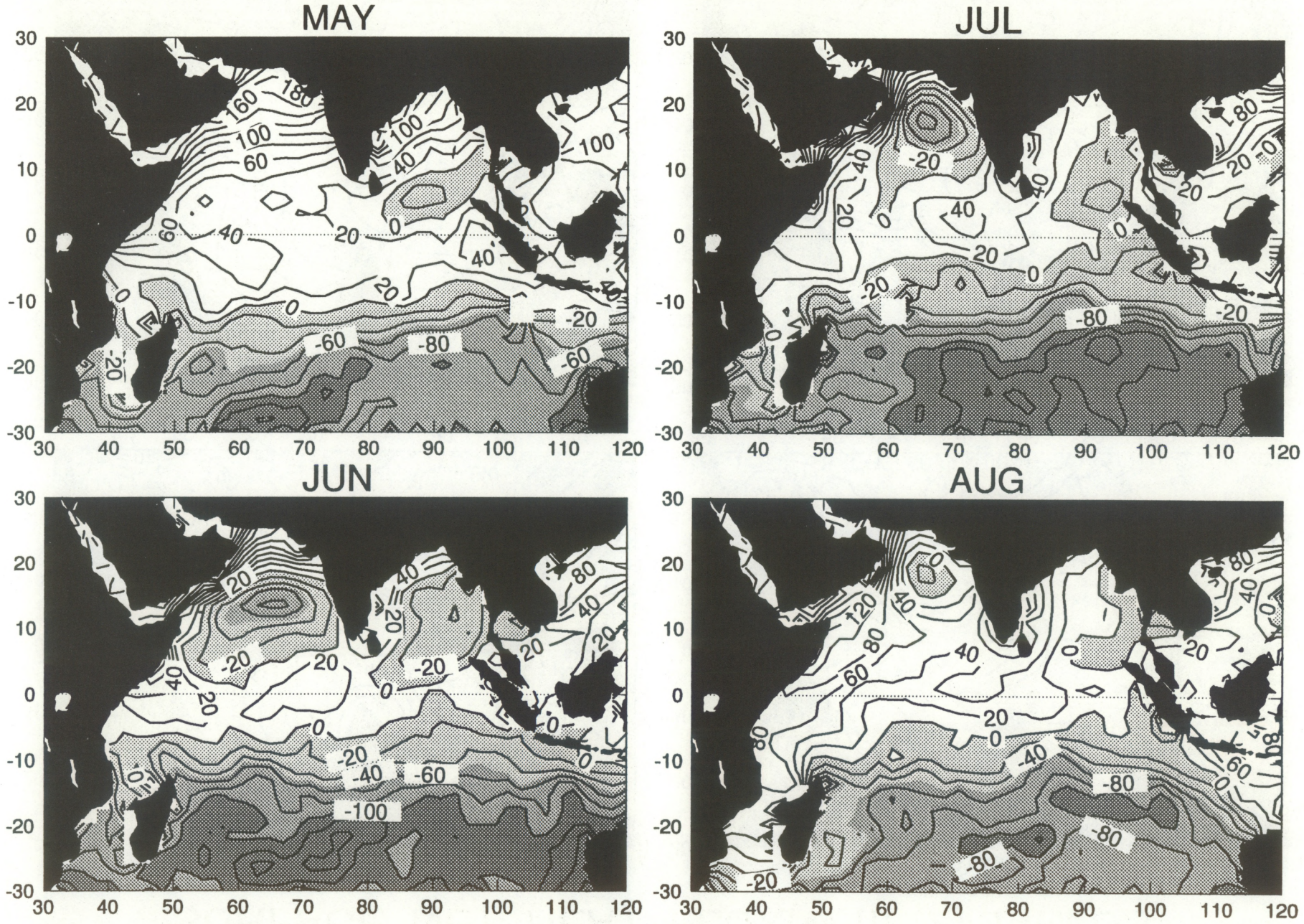

Figure 43

SURFACE NET HEAT FLUX(W/m**2) FIELDS

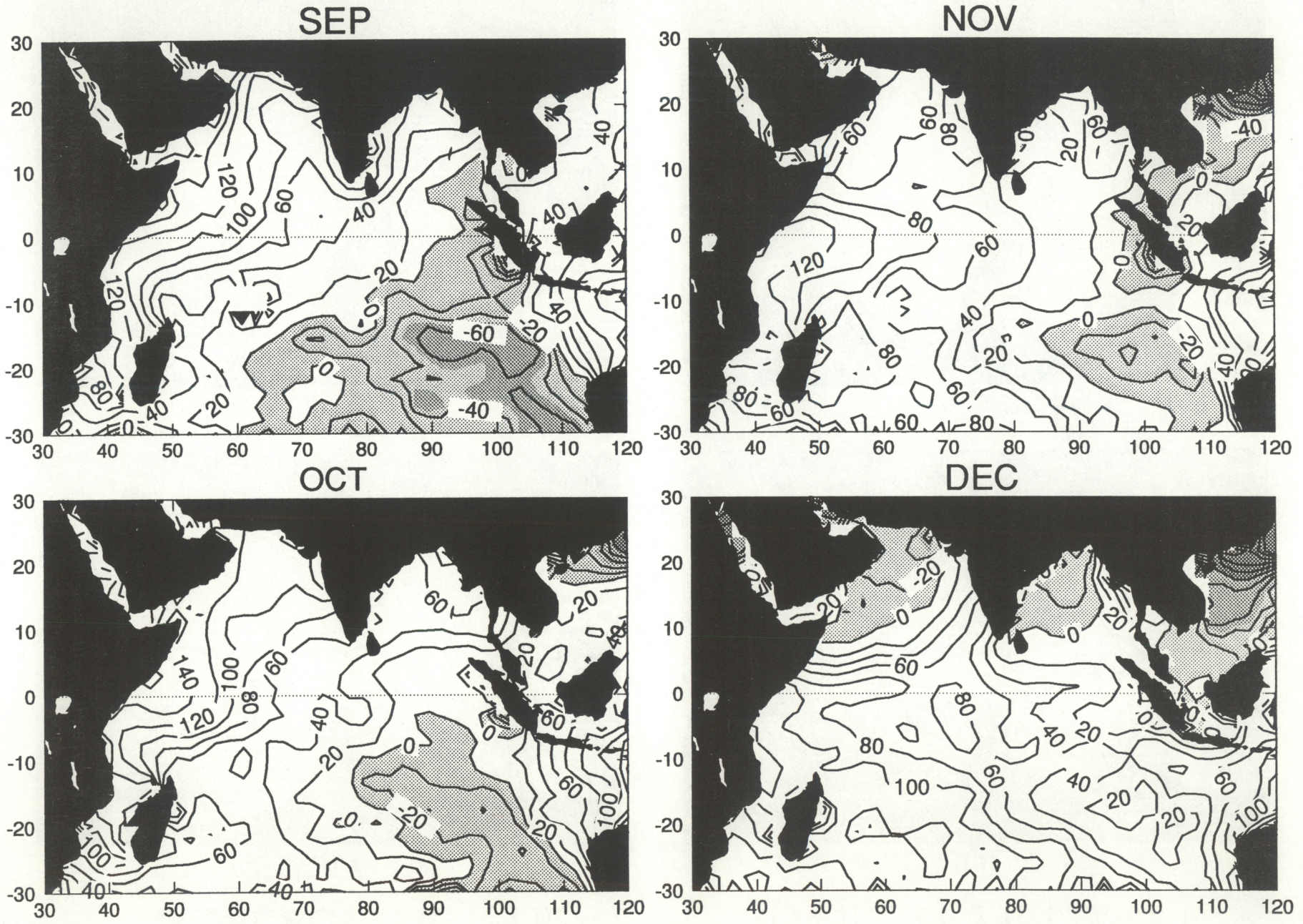

Figure 44

FOURIER FIELDS OF SEA SURFACE TEMP

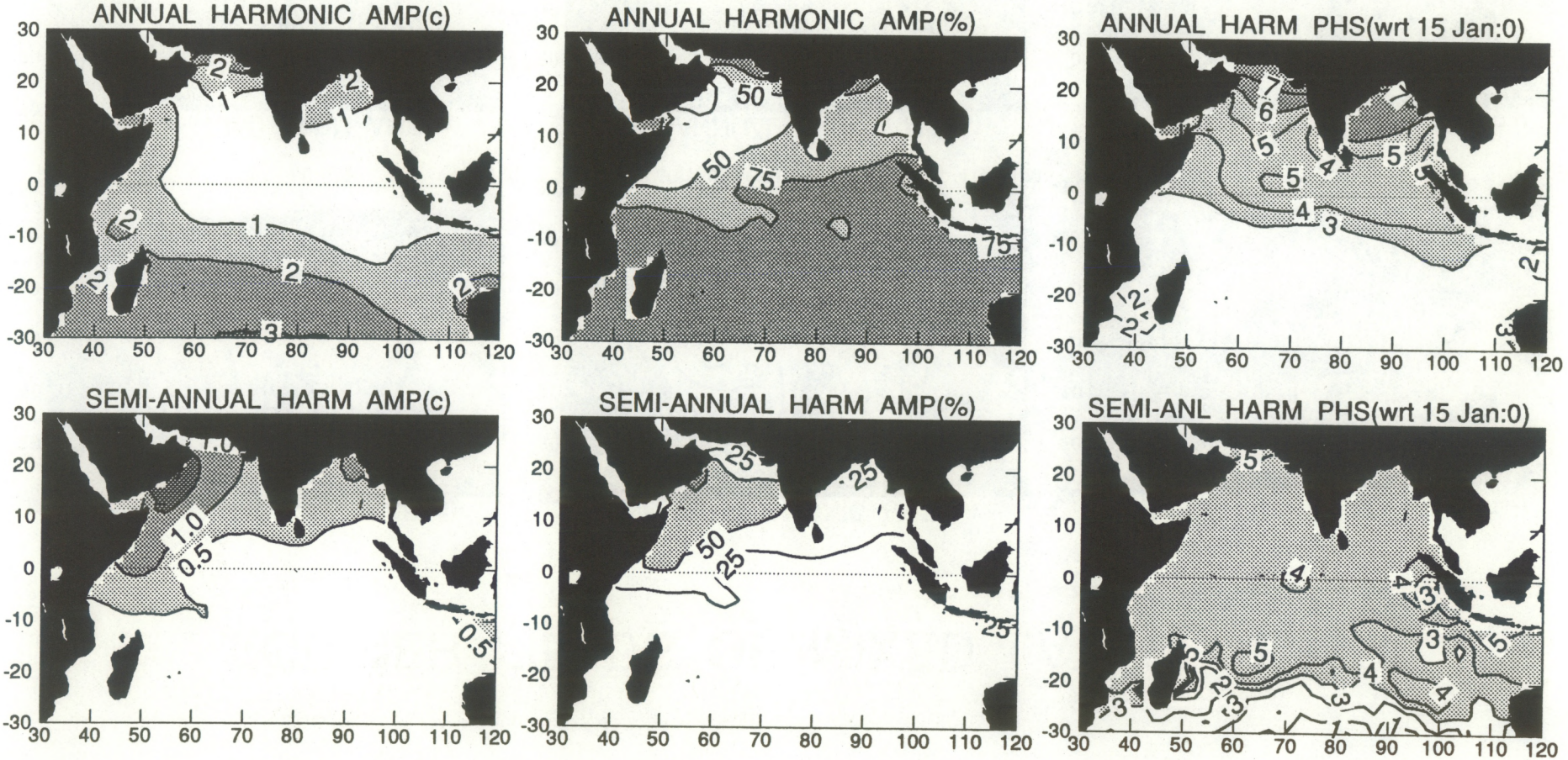

Figure 45

FOURIER FIELDS OF MIXED LAYER DEPTH

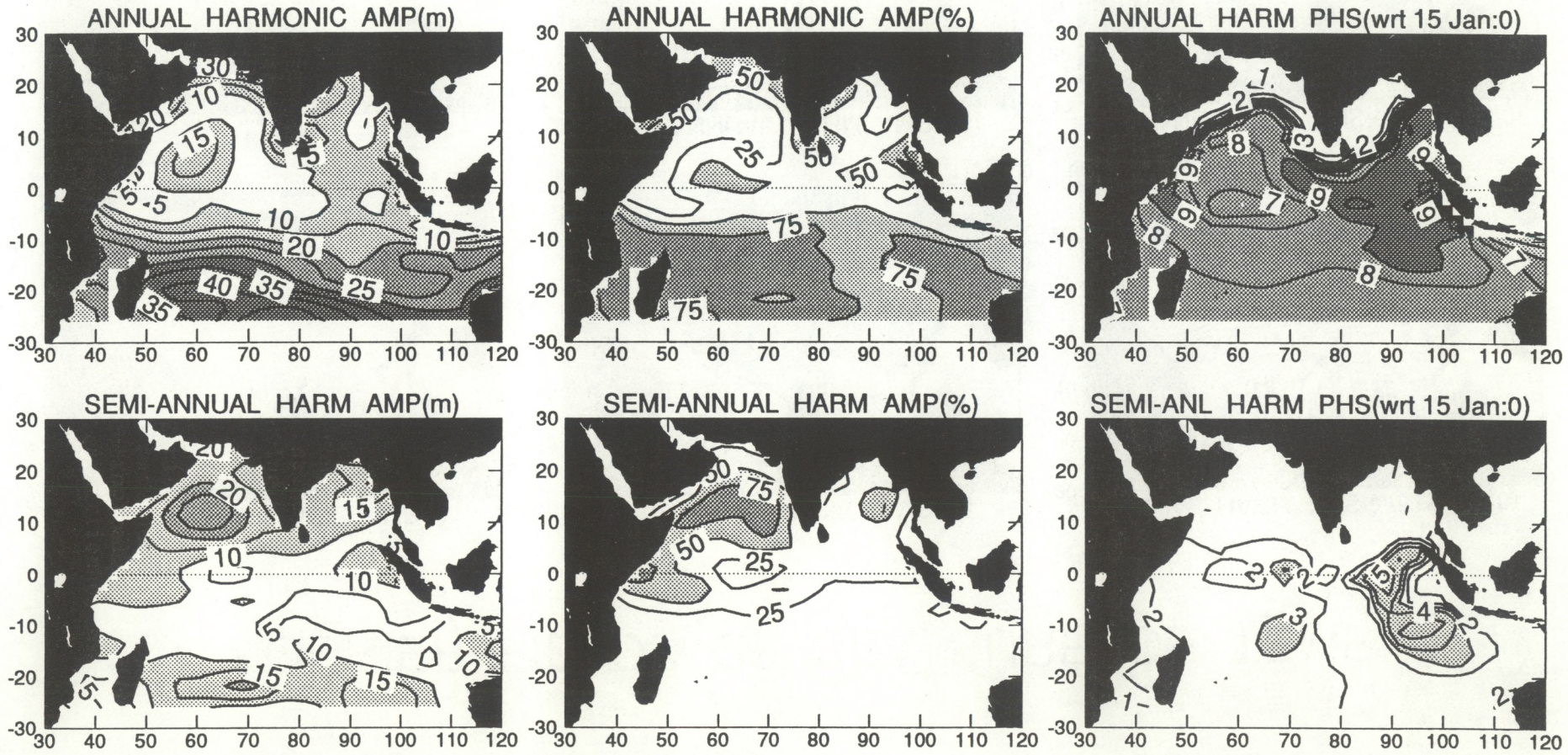

Figure 46

FOURIER FIELDS OF 20c ISOTHERM DEPTH

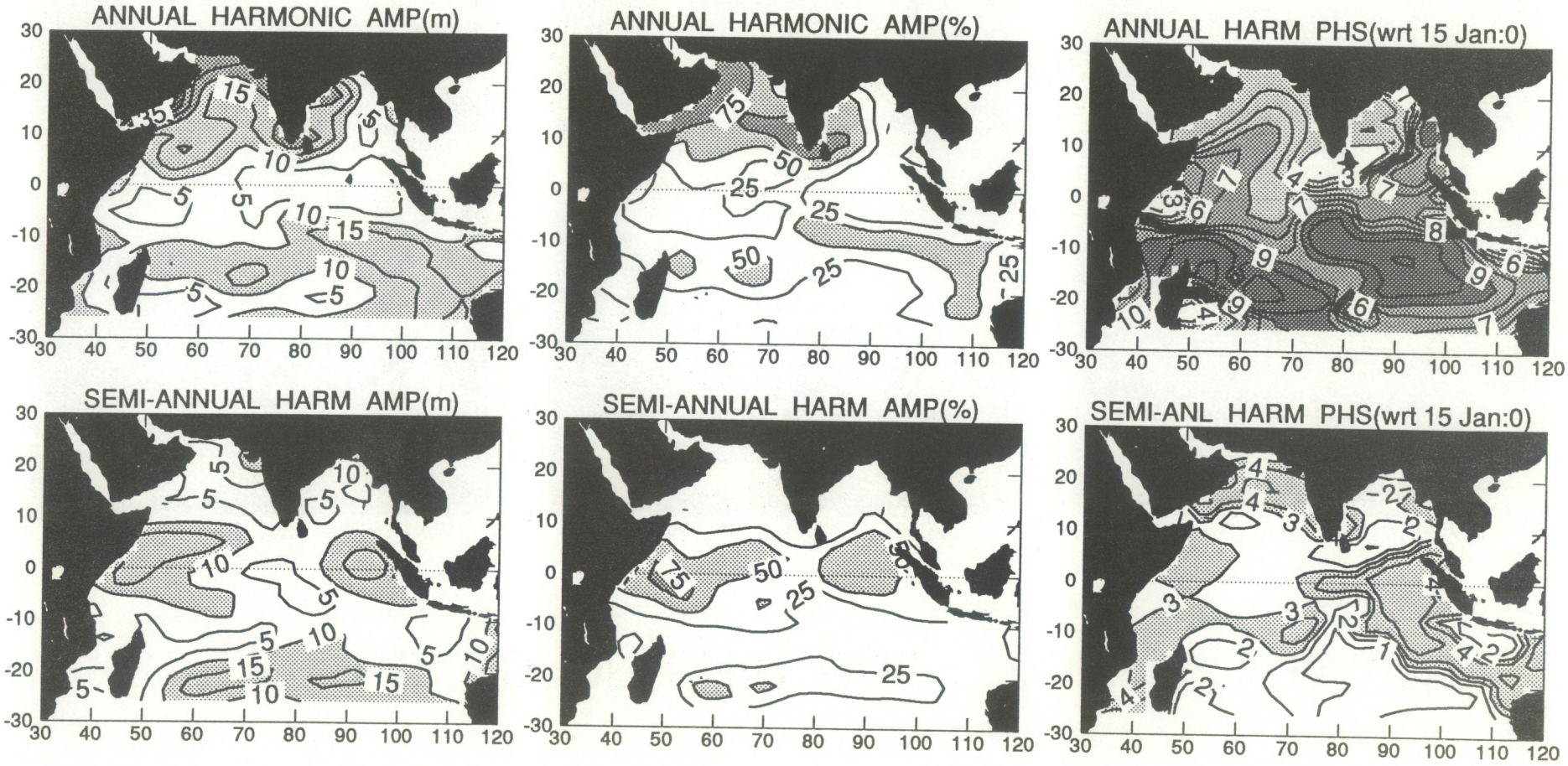

Figure 47

FOURIER FIELDS OF SHIP DRIFT ZONAL CURRENT

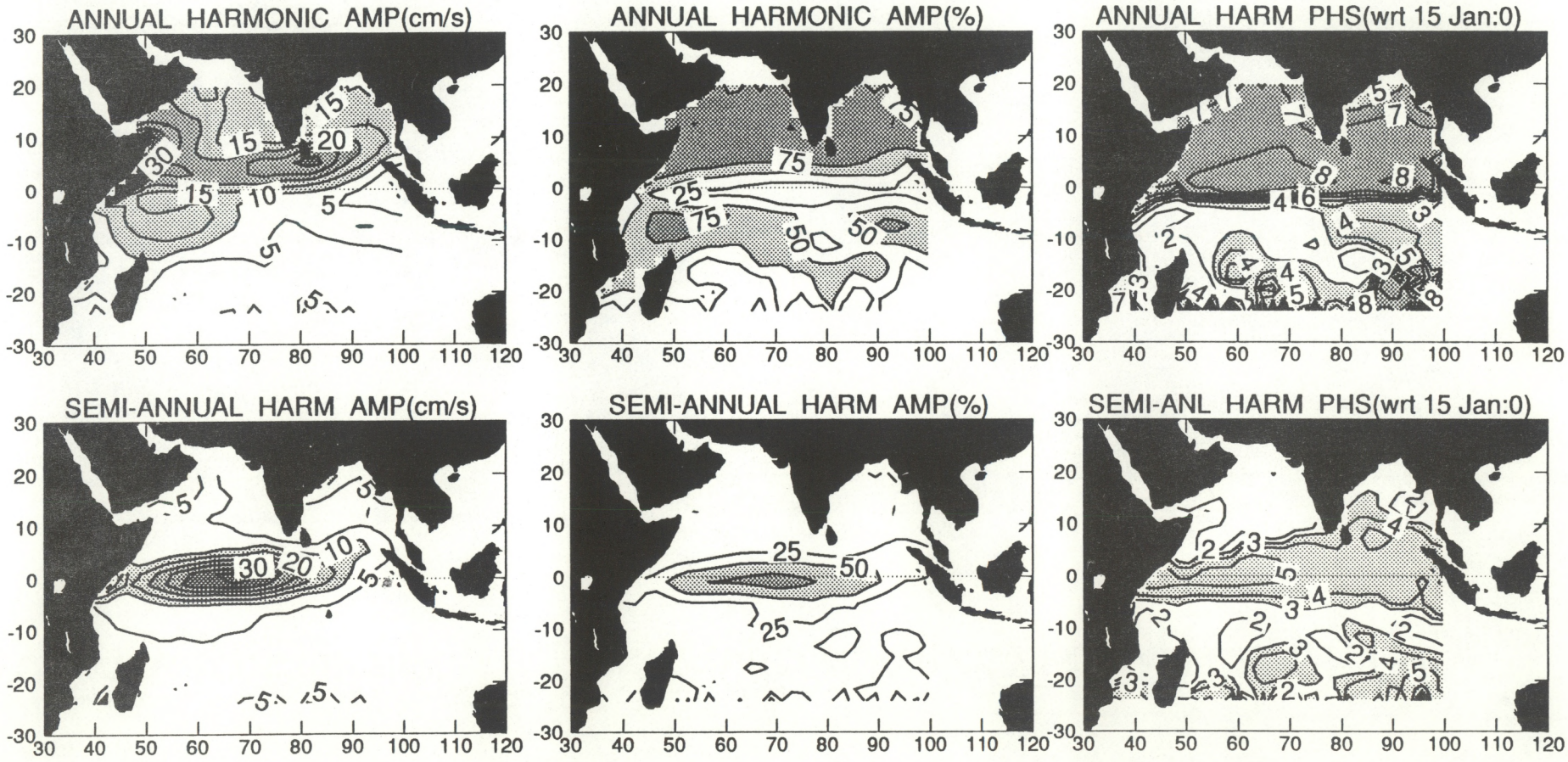

Figure 48

FOURIER FIELDS OF SHIP DRIFT MERID CURRENT

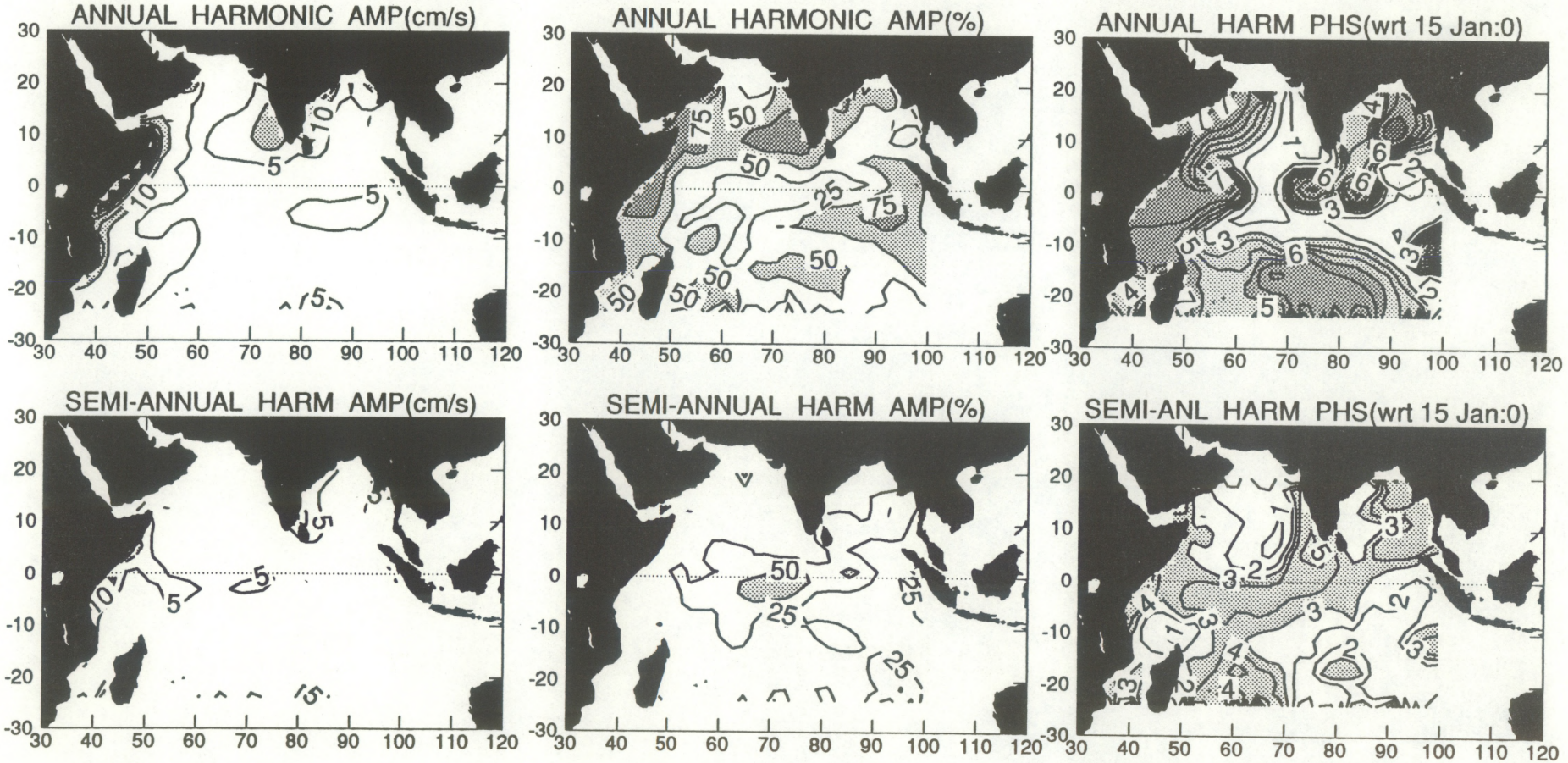

Figure 49

☆U.S. GOVERNMENT PRINTING OFFICE: 1991 - 573-002/21073